202129005

(19)中華民國智慧財產局

(12)發明說明書公開本 (11)公開編號：TW 202129005 A

(43)公開日： 中華民國 110 (2021) 年 08 月 01 日

(21)申請案號：109135798 (22)申請日： 中華民國 109 (2020) 年 10 月 15 日

(51)Int. Cl.： *C12N15/90 (2006.01)* *C12N15/11 (2006.01)*
C12N9/22 (2006.01) *A61K9/51 (2006.01)*

(30)優先權：2019/10/15 美國 62/915,143

(71)申請人：臺北榮民總醫院 (中華民國) TAIPEI VETERANS GENERAL HOSPITAL (TW)
臺北市北投區石牌路二段 201 號
國立交通大學 (中華民國) NATIONAL CHIAO TUNG UNIVERSITY (TW)
新竹市東區大學路 1001 號
國立成功大學 (中華民國) NATIONAL CHENG KUNG UNIVERSITY (TW)
臺南市東區大學路 1 號

(72)發明人：邱士華 CHIOU, SHIH-HWA (TW) ；楊添鈞 YANG, TIEN-CHUN (TW) ；張家靖 CHANG, CHIA-CHING (TW) ；曾永華 TZENG, YON-HUA (TW)

(74)代理人：鄭志玲

申請實體審查：無 申請專利範圍項數：19 項 圖式數：7 共 43 頁

(54)名稱

羧化奈米鑽石粒子媒介 CRISPR-CAS9 傳輸系統

(57)摘要

本發明提供用於基因編輯的羧化奈米鑽石粒子媒介 CRISPR-Cas9 傳輸系統，包含奈米鑽石粒子 (nanodiamond，ND)顆粒作為 CRISPR-Cas9 組分的載體，該 CRISPR-Cas9 組分被設計為在一給定基因中引入突變以修復一組織損傷。

The present invention provides a carboxylated nanodiamond -mediated CRISPR-Cas9 delivery system for gene editing comprising nanodiamond (ND) particles as the carriers of CRISPR-Cas9 components designed to introduce the mutation in a given gene for repairing a tissue damage.

指定代表圖：

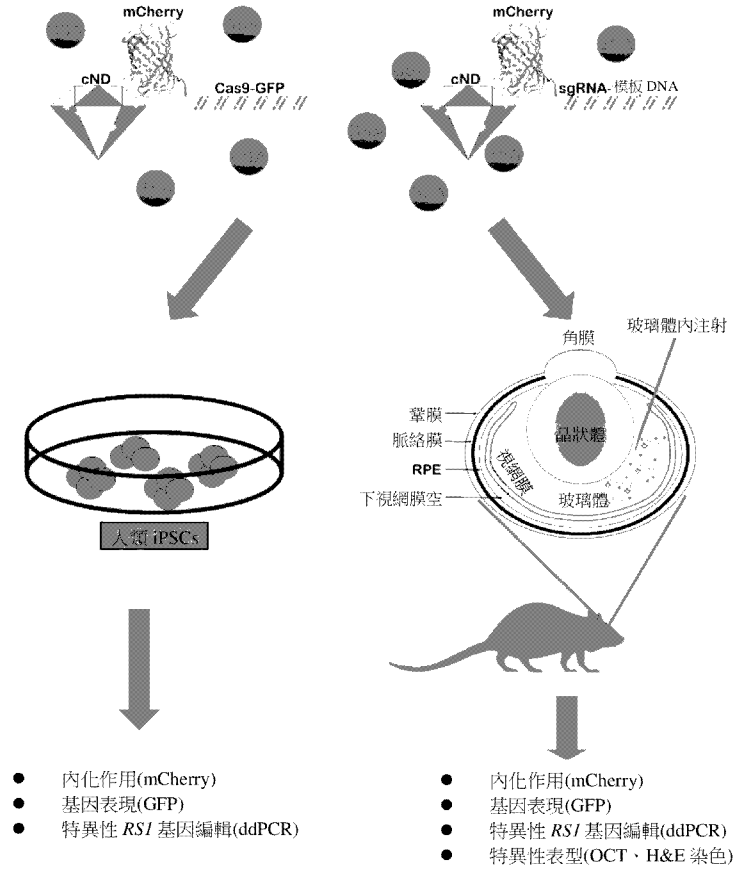
mCherry
cND
Cas9-GFP
mCherry
cND
sgRNA-模板 DNA
角膜
玻璃體內注射
鞏膜
脈絡膜
RPE
下視網膜空
晶狀體
視網膜
玻璃體
人類 iPSCs
內化作用(mCherry)
基因表現(GFP)
特異性 RS1 基因編輯(ddPCR)
內化作用(mCherry)
基因表現(GFP)
特異性 RS1 基因編輯(ddPCR)
特異性表型(OCT、H&E 染色)

【圖7】

202129005

【發明摘要】

【中文發明名稱】　羧化奈米鑽石粒子媒介CRISPR-CAS9傳輸系统

【英文發明名稱】　CARBOXYLATED NANODIAMOND-MEDIATED CRISPR-CAS9 DELIVERY SYSTEM

【中文】

本發明提供用於基因編輯的羧化奈米鑽石粒子媒介CRISPR-Cas9傳輸系統，包含奈米鑽石粒子(nanodiamond，ND)顆粒作為CRISPR-Cas9組分的載體，該CRISPR-Cas9組分被設計為在一給定基因中引入突變以修復一組織損傷。

【英文】

The present invention provides a carboxylated nanodiamond -mediated CRISPR-Cas9 delivery system for gene editing comprising nanodiamond (ND) particles as the carriers of CRISPR-Cas9 components designed to introduce the mutation in a given gene for repairing a tissue damage.

【指定代表圖】圖7

【代表圖之符號簡單說明】無

【特徵化學式】

無

【發明說明書】

【中文發明名稱】　羧化奈米鑽石粒子媒介CRISPR-CAS9傳輸系統

【英文發明名稱】　CARBOXYLATED NANODIAMOND-MEDIATED CRISPR-CAS9 DELIVERY SYSTEM

【技術領域】

【0001】 本發明涉及一種CRISPR-Cas9傳輸系統，用於傳輸一些用於治療一疾病或修復一組織損傷的組分。

【先前技術】

【0002】 X染色體串聯視網膜裂損症(X-linked juvenile retinoschisis，XLRS)為一種常見的遺傳性黃斑部病變，影響男孩的視力，患病率為1/5,000至1/25,000[1, 2]。X染色體串聯視網膜裂損症(XLRS)的臨床特徵包括與雙側中央小窩相關的早期視力喪失以及視網膜內層分裂、視網膜剝離，以及玻璃體出血[3]。*RS1*為與XLRS相關的基因，包含6個外顯子，編碼224個胺基酸的蛋白質[4]。現已確認一百多個*RS1*突變與XLRS的發展有關，且該結果也顯示高度的臨床變異性(http://www.dmd.nl/rs)。

【0003】 RS1的蛋白質結構由N端分泌前導序列以及C端區域的盤狀蛋白結構域(discoidin domain)所組成，其在物種間高度保守[5, 6]。盤狀蛋白結構域存在於許多分泌的或膜結合蛋白中，且已知與細胞黏附及細胞-細胞相互作用有關[7]。儘管也發現了無意義突變、缺失、插入，以及剪接位點突變，*RS1*基因中的大多數突變都是錯義突變[8, 9]。先前的研究顯示，在臨床上具有*RS1*錯義突變

Asp145His、Arg102Gln、Arg209His，以及Arg213Gln的患者表現出嚴重的視網膜裂損症特徵[10, 11]。RS1蛋白的錯義突變導致錯誤折疊，並可能導致細胞內及細胞外蛋白積聚，最終導致視網膜的囊狀及裂隙性結構[12]。如在小鼠視網膜中所觀察到的，RS1由外視網膜的光受體以及內視網膜的雙極細胞表現及分泌[13]。進一步的研究顯示，RS1透過光受體合成與分泌後附著在視網膜細胞表面，並調節光受體細胞、雙極細胞，以及繆氏(Müller)細胞之間的黏附，進而促進視網膜結構完整性的維持[14]。

【0004】 奈米鑽石粒子(ND)為一種基於碳的奈米材料，可用於攜帶生物分子及化學物質[15-17]。為了實現奈米鑽石粒子多功能傳輸之目的，已經開發了幾種技術以透過引入羧基、羥基，以及硫醇基團來促進化學物質與表面的結合。許多研究報告指出，奈米鑽石粒子也可作為生物分子的傳遞系統，例如DNA [18, 19]、蛋白質[20, 21]，以及小分子藥物[22, 23]。奈米鑽石粒子的生物相容性及無毒性使其成為用於生物醫學應用上相對安全的奈米材料[24]。奈米鑽石粒子的這些優點使其有希望成為治療遺傳性視網膜疾病的治療劑載體。

【0005】 奈米鑽石粒子在人類疾病治療中的應用前景廣闊，但美國食品暨藥品監督管理局(Food and Drug Administration，FDA)仍要求注入體內的藥物不能長時間積聚[25]。儘管螢光標記的奈米鑽石粒子具有穩定螢光訊號的優勢，但仍需要更大的粒徑才能保持螢光敏感性[26]。動物實驗發現，即使沒有明顯的毒性，較大的顆粒也可能在器官中積聚[27, 28]。奈米顆粒的周轉是臨床應用上的重要問題。腎臟產生的尿液是消除奈米顆粒的重要方法[29]。無機奈米顆粒透過腎小球毛細血管壁過濾分子的閾值約為5.5 nm。因此，奈米鑽石粒子的大小可能會影響腎臟清除的效率[30]。

【0006】期望開發使用安全、有效，以及可追蹤的奈米載體之傳輸系統。

【發明內容】

【0007】因此，本發明提供一種用於基因編輯的高效傳輸系統。

【0008】於一方面，本發明提供一種用於基因編輯的傳遞系統，包含奈米鑽石粒子顆粒作為CRISPR-Cas9組分的載體，該CRISPR-Cas9組分包括一Cas9蛋白、一引導蛋白(gRNA)、一設計用於將一突變引入一給定基因以修復一組織損傷的模板DNA，其中該奈米鑽石粒子顆粒的直徑小於5 nm，且透過其表面的羧化作用而官能化並與一螢光蛋白共價結合；以及一用於表現該Case 9蛋白的第一線性DNA構築體以及一用於表現該gRNA/模板DNA的第二線性DNA構築體透過磷醯咪唑與該共價結合至該螢光蛋白的奈米鑽石粒子顆粒連接以獲得羧化奈米鑽石粒子媒介CRISPR- Cas9奈米鑽石顆粒。

【0009】於本發明之一實施例中，該奈米鑽石粒子顆粒的直徑在3 nm-5 nm的範圍內；較佳地，該奈米鑽石粒子顆粒的直徑為約3 nm。

【0010】於一實施例中，本發明中使用之螢光蛋白為mCherry蛋白。

【0011】於一特定實施例中，根據本發明之羧化奈米鑽石粒子媒介CRISPR-Cas9奈米鑽石顆粒可在使用前以牛血清白蛋白(bovine serum albumin，BSA)包覆。令人意外地發現，奈米鑽石粒子的傳輸效率增加，且mCherry螢光點的直徑減小，表示較少聚集狀態。

【0012】於一實施例中，該給定基因為與X染色體串聯視網膜裂損症(XLRS)相關的*RS1*基因。

【0013】 根據本發明創造之一疾病模型，該給定基因中的突變為經由兩個線性DNA構築體引入的，該線性DNA構築體與該結合的mCherry連接，且該第一線性DNA構築體編碼Cas9核酸內切酶以及一綠色螢光蛋白(green fluorescent protein，GFP)報導基因，且該第二線性DNA構築體編碼一sgRNA，並包含一HDR模板的插入片段，該插入片段設計用於引入*RS1* c.625C> T突變。

【0014】 於本發明中，該傳輸導致將*RS1* c.625C> T突變引入人類誘導性多能幹細胞(induced pluripotent stem cells，iPSCs)或小鼠視網膜中。

【0015】 於另一方面，本發明提供一種用於治療一個體的一疾病或修復一組織損傷的方法，包含透過本發明之系統將一給定基因中的突變傳輸並內化到該個體中。

【0016】 於一實施例中，該疾病為X染色體串聯視網膜裂損症(XLRS)，且該給定基因為與X染色體串聯視網膜裂損症(XLRS)相關的*RS1*基因。

【0017】 於另一方面，本發明提供一種用於創造體外或體內疾病模型之方法，該方法包含透過本發明之系統將一給定基因中的突變傳輸並內化到誘導性多能幹細胞(iPSCs)或一動物器官中。

【0018】 於一實施例中，該疾病為X染色體串聯視網膜裂損症(XLRS)，該給定基因為與X染色體串聯視網膜裂損症(XLRS)相關的*RS1*基因，且該動物器官為小鼠視網膜。

【0019】 於本發明之一實施例中，該傳輸導致將*RS1* c.625C> T突變引入人類誘導性多能幹細胞(iPSCs)或小鼠視網膜。

【0020】 根據本發明，在該小鼠視網膜中編輯的該*Rs1*基因導致幾種X染色體串聯視網膜裂損症(XLRS)典型的病理特徵，例如異常的光受體結構。

【0021】 應當理解的是，以上的一般描述以及以下的詳細描述都僅為示例性及說明性的，並不限制本發明。

【圖式簡單說明】

【0022】 當結合附圖閱讀時，將更好地理解前述發明內容及以下對本發明之詳細描述。為了說明本發明，在附圖中示出了目前較佳的具體實施例。

【0023】 於圖式中：

【0024】 圖1A、圖1B，以及圖1C所示為具有X染色體串聯視網膜裂損症(XLRS)的*RS1* c.625C> T突變攜帶者患者的臨床特徵。圖1A所示為正常個體(頂圖)以及XLRS患者(底圖)中突變的*RS1*基因座的Sanger定序結果。*RS1*外顯子6中的c.625C> T突變導致精胺酸變為半胱胺酸。圖1B提供XLRS患者眼睛的眼底鏡檢查影像，所示為包括中央小窩的脈絡膜網萎縮的清晰區域。圖1C提供了光學同調斷層掃描(optical coherence tomography，OCT)影像，顯示指示該視網膜變性的大囊腫的存在。

【0025】 圖2A-圖2E所示為CRISPR-Cas9構築體的設計，以引入*RS1*突變以及mCherry標記的奈米鑽石粒子的功能化以用於其傳輸。圖2A提供顯示將c.625C> T突變引入人類*RS1*基因的CRISPR-Cas9構築體的設計之示意圖。*RS1*外顯子6序列的片段包含上方所示的切割位點(紅色箭頭)及PAM序列(紅色字體)。底部所示為兩個DNA構築體，*Cas9-GFP*以及*RS1-sgRNA*的圖譜。圖2B提供顯示設計及生產裝載CRISPR-Cas9的奈米鑽石粒子之方案，其中在EDC催化的反應中，羧化奈米鑽石粒子(carboxylated NDs，cNDs)經由COOH基團共價連接到mCherry，以產生cND-mC、*Cas9-GFP*及*RS1-sgRNA*線性DNA透過His-tag與cND-

mC連接，產生cND-mC-C/C9。圖2C提供與mCherry偶聯的羧化奈米鑽石粒子的明亮視圖及螢光顯微圖像。圖2D所示為瓊脂糖凝膠，其顯示未偶聯及奈米鑽石粒子偶聯的*Cas9-GFP*以及*RS1-sgRNA* DNA構築體的遷移。圖2E提供奈米鑽石粒子樣品的FTIR光譜：羧化奈米鑽石粒子(綠線)、cND-mC (藍線)，以及cND-mC-C/C9 (棕線)。圖2F提供BSA混合的cND-mC-C/C9奈米顆粒的TEM影像。

【0026】 圖3A-圖3E提供在hiPSC中cND-mC-C/C9對*RS1*基因的編輯。圖3A提供以混合所示濃度的BSA的cND-mC-C/C9奈米顆粒處理的hiPSCs的螢光顯微影像。圖3B所示為使用ImageJ軟體在螢光顯微鏡影像上測量hiPSC內的mCherry螢光點的直徑。以標準偏差誤差線顯示平均值。圖3C所示為與不同濃度的BSA混合的cND-mC-C/C9奈米顆粒的傳輸效率的定量。表示為具有內在mCherry訊號的細胞的平均百分比。圖3D提供以cND-mC-C/C9處理的hiPSC的GFP分選群體中*RS1* c.625C> T複製數的ddPCR分析。圖3E提供CCK-8細胞活力測定的結果，顯示以指定濃度的cND-mC-C/C9處理hiPSCs的效果影響了它們的活力(數據表示為相對於未處理組(0 μg/ml)。統計數據顯示為平均值±標準偏差誤差線，* p <0.05，*** p <0.001，## p <0.01 來自3個獨立實驗的學生氏t檢驗。* 相較於0% BSA、# 3% BSA相較於1% BSA)。

【0027】 圖4A-圖4D所示為將cND-mC-C/C9傳輸到小鼠視網膜中。圖4A提供注射有攜帶*Cas9-GFP* (僅Cas9)以及*RS1-sgRNA* (Cas9 + sgRNA) DNA構築體的cND-mC-C/C9奈米顆粒的小鼠眼中的SLO眼底影像。圖4B提供在cND-mC-C/C9處理的小鼠視網膜的橫截面中mCherry以及綠色螢光蛋白(green fluorescent protein，GFP)訊號的定位的螢光顯微鏡觀察。GFP及mCherry訊號由箭頭指示。圖4C提供以cND-mC-C/C9處理的小鼠視網膜的橫截面中GFP表現的表現螢光顯

微鏡觀察。在RGC層(黃色箭頭)、光受體/繆氏細胞層(紅色箭頭)，以及RPE層(白色箭頭)中觀察到GFP訊號。恢復素為光受體的標記物，以紅色免疫染色。細胞核以DAPI染色。圖4D提供以cND-mtwC-C/C9處理的小鼠視網膜的切片的H&E染色。RPE (retinal pigment epithelium) –視網膜色素上皮，PR (photoreceptors) –光受體，ONL (outer nuclear layer) –外核層，OPL (outer plexiform layer) –外網狀層，INL (inner nuclear layer) –內核層，IPL (inner plexiform layer) –內網狀層，RGC (retinal ganglion cells) –視網膜神經節細胞。

【0028】 圖5A-圖5D所示為cND-mC-C/C9在小鼠視網膜中對*Rs1*基因的編輯。圖5A提供顯示將c.625C> T突變引入小鼠*Rs1*基因的CRISPR-Cas9構築體的設計方案。*Rs1*外顯子6序列片段包含在頂部顯示的切割位點(紅色箭頭)以及PAM序列(紅色字體)。底部所示為兩個DNA構築體*Cas9-GFP*以及*Rs1-sgRNA*的圖譜。圖5B所示為以對照(僅Cas9)以及以*Rs1*為目標的cND-mC-C/C9奈米顆粒(Cas9 + sgRNA)處理兩週的視網膜中*Rs1* c.625C> T複製數的ddPCR分析結果。數據表示為相對於對照。圖5C提供以對照(僅Cas9)以及(Cas9 + sgRNA) cND-mC-C/C9奈米顆粒處理兩週的小鼠視網膜的OCT影像。右側顯示的視網膜層：GCL (ganglion cell layer) –神經節細胞層，IPL –內網狀層，INL –內核層，ONL –外核層，OPL –外網狀層，OLM (outer limiting membrane) –外限界膜，IS (inner segments) –內層部分，OS (outer segments) –外層部分，RPE –視網膜色素上皮。下圖：放大以紅色矩形包圍的上圖區域，顯示高反射性外部視網膜帶2及3的結構。圖5D提供圖4C的OCT影像中的高反射性外部視網膜帶2及3的厚度的量化。表示為平均值測量的數據，相對於「僅Cas9」對照定量「Cas9 + sgRNA」。圖5E提供以對照(僅Cas9)以及(Cas9 + sgRNA) cND-mC-C/C9奈米顆粒處理兩週的小鼠視網膜的橫截

面的H&E染色。圖5F所示為圖5E中的OCT影像中的IS/OS層的厚度的量化。數據表示為來自3次測量的平均值，相對於「僅Cas9」對照定量「Cas9 + sgRNA」。

【0029】 圖6A-圖6C所示為cND-mC-C/C9媒介*Rs1*編輯對小鼠視網膜中的光受體細胞的影響。以對照cND-mC-C/C9顆粒(僅Cas9)以及以*Rs1*基因為目標(Cas9 + sgRNA)的cND-mC-C/C9顆粒處理過的小鼠視網膜的橫截面進行免疫螢光染色。右側指示的視網膜層：IPL –內網狀層，INL –內核層，OPL –外網狀層，ONL –外核層，IS –內層部分，OS –外層部分。以DAPI標記核。圖6A所示為以針對視錐細胞特異性視蛋白(Opsin)以及RS1的抗體進行的免疫染色。圖6B所示為以針對恢復蛋白及視紫紅質的抗體進行的免疫染色。圖6C所示為視錐細胞特異性視蛋白的免疫螢光訊號的長度之定量。

【0030】 圖7所示為該研究之總結，其中奈米鑽石粒子被功能化以共價連接mCherry蛋白及編碼CRISPR-Cas9基因組編輯系統的組分的DNA構築體。將奈米粒子與BSA混合，並用於編輯iPSCs及小鼠視網膜的基因組，進而使它們成為分別創造體外及體內疾病模型的有用工具。

【實施方式】

【0031】 除非另有定義，否則本文使用的所有技術及科學術語具有與本發明所屬領域的技術人員通常理解的相同含義。

【0032】 奈米鑽石粒子(ND)顆粒可作為具有高生物相容性、負載能力，以及細胞穿透性的藥物輸送載體。奈米鑽石粒子-寡核苷酸結合的非共價方法可用於製備奈米鑽石粒子，且該核酸透過胜肽的共價鍵有助於結合物的穩定性、可及性，以及選擇性。於本發明中，透過以下方式設計基於奈米鑽石粒子的CRISPR-

Cas9傳輸載體：以一羧基(COOH)基團使奈米鑽石粒子表面官能化、將6His-tag標記的mCherry報導蛋白透過胜肽鍵結合至該奈米鑽石粒子，以及透過DNA的5’-磷酸與6His-tag標記的組胺酸的咪唑基團之間的磷醯咪唑鍵共價連接編碼綠色螢光蛋白(GFP)報導蛋白的線性DNA以及CRISPR-Cas9系統的組份。由於奈米粒子的內化通常是透過胞內體途徑進行的，因此選擇mCherry來構築傳輸載體的骨架以監測轉染效率，因為即使在晚期胞內體的酸性環境(pH 5-6)中，它也能構成紅色螢光，而與綠色螢光蛋白(GFP)不同，綠色螢光蛋白(GFP)的綠色螢光在這樣的pH值下被淬滅。同時，綠色螢光蛋白(GFP)被設計為從一結合的DNA中表現，作為運送的DNA成功傳遞及功能作用的報導基因。

【0033】 如本文所用，「奈米鑽石粒子(ND)」，「奈米鑽石粒子(ND)顆粒」或「鑽石奈米顆粒」等詞係指具有小於1 μm尺寸的菱形的顆粒，其可透過例如爆炸或隕石撞擊等撞擊事件產生，可能會導致表面官能化。由於廉價、大規模合成，其具有表面官能化的潛力。奈米鑽石粒子顆粒可作為具有高生物相容性、負載能力，以及細胞滲透性的藥物/生物材料輸送載體。奈米鑽石粒子-寡核苷酸結合的非共價方法可用於製備奈米鑽石粒子，且該核酸透過該胜肽的共價鍵有助於結合物的穩定性、可及性，以及選擇性。

【0034】 於本發明之一個實施例中，透過以下方式設計基於奈米鑽石粒子的CRISPR-Cas9傳輸載體：以一羧基(COOH)基團使奈米鑽石粒子表面官能化、將6His-tag標記的mCherry報導蛋白透過胜肽鍵結合至該奈米鑽石粒子，以及透過DNA的5’-磷酸與6His-tag標記的組胺酸的咪唑基團之間的磷醯咪唑鍵共價連接編碼綠色螢光蛋白(GFP)報導蛋白的線性DNA以及CRISPR-Cas9系統的組份。由於奈米鑽石粒子顆粒的內化通常是透過胞內體途徑進行的，因此選擇mCherry

來構築傳輸載體的骨架以監測轉染效率，因為即使在晚期胞內體的酸性環境(pH 5-6)中，它也能構成紅色螢光，而與綠色螢光蛋白(GFP)不同，綠色螢光蛋白(GFP)的綠色螢光在這樣的pH值下被淬滅。同時，綠色螢光蛋白(GFP)被設計為從一結合的DNA中表現，作為運送的DNA成功傳遞及功能作用的報導基因。我們證明羧化奈米鑽石粒子攜帶的mCherry蛋白在小鼠視網膜中穩定長達兩週。此外，綠色螢光蛋白(GFP)報導基因也從質體DNA體內連續表現。為了確保透過奈米載體進行更有效的轉染，通常需要用其他材料穩定它們。

【0035】 於本發明中發現，牛血清白蛋白(bovine serum albumin，BSA)以濃度相依的方式增加了羧化奈米鑽石粒子的傳輸效率，並且減小了mCherry螢光點的直徑，顯示聚集狀態較少(參見圖3)。

【0036】 CRISPR-Cas9媒介多能幹細胞的基因組編輯，包括胚胎幹細胞(embryonic stem cells，ESCs)以及誘導性多能幹細胞(induced pluripotent stem cells，iPSCs)，為人類遺傳疾病的模型的建立提供極大的潛力，因為它們可分化為受病理影響的任何組織 。於本發明中，基於羧化奈米鑽石粒子(cND)的方法可用於將CRISPR-Cas9組分安全有效地傳輸至人類誘導性多能幹細胞(iPSCs)。透過使用我們的cND-mC-C/C9傳遞系統，我們可成功地將X染色體串聯視網膜裂損症(XLRS)特異性的*RS1*基因突變(c.625C> T)引入正常人類誘導性多能幹細胞(iPSCs)。將來，此類敲入式誘導性多能幹細胞(iPSCs)可透過將其分化為3D視網膜類器官並使用具有相同遺傳背景的父母的誘導性多能幹細胞(iPSCs)作為對照來研究視網膜病變的分子及細胞機制。

【0037】 X染色體串聯視網膜裂損症(XLRS)是由*RS1*基因突變引起的X染色串聯視網膜裂損症，其特徵為視網膜層分裂。在以前表徵的*Rs1*基因敲除小鼠

模型中證實幾種病理特徵，包括核外層(outer nuclear layer，ONL)厚度減少以及視網膜內空化。於本發明中，經cND-mC-C/C9奈米粒子處理的小鼠視網膜的OCT成像未顯示視網膜中存在囊腫，但是，我們清楚地觀察到高反射性外部視網膜帶2及3合併，顯示異常的光受體結構。一致地，對視網膜組織切片的分析顯示視網膜外層厚度的減少及光受體細胞的形態縮短。製備成年雄性小鼠的部分人類突變體*Rs1*基因，以顯示光受體細胞外段變化的表型，這支持了*Rs1*基因喪失活性可能直接引起光受體細胞損傷的想法。玻璃體內注射導致所有視網膜細胞類型均暴露於奈米鑽石粒子，但只有感光層的形態受其影響，因此證實了RS1蛋白的功能特異性為組織外部視網膜的關鍵因素。另一方面，透過使用此載體設計的優勢，可潛在地提高我們基於奈米鑽石粒子的載體針對特定細胞類型，如光受體細胞的特異性。當我們使用羧化奈米鑽石粒子的COOH基團透過胜肽鍵將mCherry報導分子標記共價連接時，細胞類型的特異性配體蛋白可同時結合，使奈米鑽石粒子以感光受體特異性表面標記為目標。

【0038】 相較於基於病毒的系統，基於奈米鑽石粒子的載體的缺點為轉染效率低，而其優勢是基於作為惰性及低免疫原性材料的更高安全性。透過使用掃描雷射光眼底鏡檢查，我們觀察到玻璃體內注射奈米鑽石粒子後綠色螢光蛋白(GFP)訊號在小鼠視網膜中持續存在長達12天(圖3A)。因此，鑑於奈米鑽石粒子的更高安全性，我們可以推測，一旦綠色螢光蛋白(GFP)訊號減弱，透過注入奈米鑽石粒子來保持恆定的高濃度，可以提高體內基因組編輯的效率。

【0039】 透過以下實施例進一步說明本發明，提供這些實施例是為了說明而非限制。

【0040】 **實施例**

【0041】 1.1. CRISPR-Cas9設計

【0042】 在先前的研究中描述Cas9-GFP表現載體[31]。使用以下sgRNA支架序列引入人類*RS1* c.625 C> T (p.R209C)突變：

GGCACGTCTGCATTGCCATCGTTTTAGAGCTAGAAATAGCAAGTTAAAAT

AAGGCTAGTCCGTTATCAACTTGAAAAAGTGGCACCGAGTCGGTGC (SEQ ID NO: 1)；

以及以下HDR序列：

GTCTTCTATGGCAACTCGGACCGCACCTCCACGGTTCAGAACCTGCTGCG

GCCCCCCATCATCTCCCGCTTCATCCGCCTCATCCCGCTGGGCTGGCATGT

CCGGATTGCCATCCGGATGGAGCTGCTGGAGTGCGTCAGCAAGTGTGCCT

GATGCCTGCCTCAGCTCGGCGCCTGCCAGGGGGTGACTG (SEQ ID NO: 2)。

【0043】 使用sgRNA支架序列引入小鼠*Rs1* c.625 C> T：

GGCATGTCCGAATTGCCATCGTTTTAGAGCTAGAAATAGCAAGTTAAAAT

AAGGCTAGTCCGTTATCAACTTGAAAAAGTGGCACCGAGTCGGTGC (SEQ ID NO: 3)；

以及HDR序列：

GTCTTCTATGGAAACTCAGACCGGAGTTCTACAGTTCAGAACTTACTCAG

GCCCCCCATCATTTCCCGCTTCATCCGACTGATCCCTCTAGGCTGGCAcGT

CtGtATTGCCATCCGGATGGAGCTGCTTGAGTGTGCCAGCAAGTGTGCCTG

ATGTCTATTTCAGCTCAGTTCTGTCACTTGCAGGGAGA (SEQ ID NO: 4)。

【0044】 將sgRNA支架與HDR序列選殖至pUC57載體(Addgene公司)中。

【0045】 1.2. 羧化奈米鑽石粒子(cND)的製備以及與mCherry及線性DNA連接

【0046】爆轟奈米鑽石粒子以2.5% (w/v)水膠體溶液的形式購自NanoCarbon Institute有限公司。根據提供的膠體溶液的規格，它包含尺寸分佈在3.2 ± 0.6 nm左右的顆粒。石墨烯在奈米鑽石粒子表面形成並存在氧化鋯微珠及引爆室產生的金屬離子的微小污染，但對這項研究的危害很小或沒有危害。為了使帶有羧基(COOH)的奈米鑽石粒子表面官能化，將它們以3：1的H_2SO_4以及HNO_3混合物於100°C下攪拌處理72小時。將所得的羧化奈米鑽石粒子(cNDs)在二次蒸餾水中洗滌幾次，並以250 μg/ml的濃度懸浮於PBS中。mCherry蛋白透過以1-乙基-3-(3-二甲基胺基丙基)碳二亞胺(1-ethyl-3-(3-dimethylaminopropyl)carbodiimide，EDC)為催化劑的胜肽與羧化奈米鑽石粒子連接。將羧化奈米鑽石粒子(在PBS中的250 μg/ml懸浮液)、mCherry蛋白(250 μg/ml)，以及0.1 M ECD以1：2：3的體積比混合，並於4°C下在搖床上作用18小時。透過以PBS透析18小時來純化反應產物(cND-mCherry)。mCherry與線性DNA透過mCherry 6His-tag尾部的咪唑基團以及DNA磷酸基團之間的磷醯咪唑鍵連接。將cND-mCherry PBS溶液(大約40 μg/ml)、線性化的DNA構築體(200 μg/ml)，以及0.1 M ECD以5：2：1的體積比混合，並於4°C下在搖床上作用18小時。透過以PBS透析18小時來純化反應產物。在將負載的奈米鑽石粒子應用於細胞之前，添加終濃度為1%或3% (w/v)的牛血清白蛋白(BSA)，並以音波震動處理奈米顆粒2小時，以防止其聚集並確保均勻分配。

【0047】1.3. 穿透式電子顯微鏡(Transmission electron microscopy，TEM)以及傅立葉轉換紅外光譜(Fourier transform infrared spectroscopy，FTIR)

【0048】在100 kV的JEM-2000EX II (JEOL公司)上獲得奈米鑽石粒子的TEM影像。將奈米鑽石粒子(40 μg/mL)懸浮於PBS中，然後將其吸移到銅TEM網

格(Ted Pella公司)上，過夜沉積後去除溶劑。使用FT/IR-4200光譜儀(JASCO公司)透過FTIR檢測奈米鑽石粒子的表面修飾，掃描尺寸(解析度)為4 cm^{-1}，每個樣品掃描256次。

【0049】 1.4 人類誘導性多能幹細胞(iPSCs)

【0050】 如前所述，人類誘導性多能幹細胞(iPSCs)是透過從健康的男性漢族捐贈者的周邊血單核細胞(peripheral blood mononuclear cells，PBMCs)重新編程生成的。簡言之，將周邊血單核細胞(PBMCs)接種在含有完全PBMC培養基的24孔盤中(5 x 10^5細胞/孔)。以感染度(multiplicity of infection，MOI)為3將編碼OCT3/4、SOX2、KLF4，以及cMYC的SeV載體混合物轉導至周邊血單核細胞(PBMCs)。每隔一天更換一次培養基，轉導後第7天，將1.25 x 10^5個細胞塗在預先塗有小鼠胚胎纖維母細胞(mouse embryonic fibroblast，MEF)滋養層的10 cm培養皿上。於第二天，將培養基更換為hES培養基，且每隔一天飼餵細胞持續7天，然後轉換為每日飼餵。選殖株出現後，將其機械移位並轉移到新鮮的滋養層上。將hiPSCs在Geltrex包覆的細胞培養皿上培養與mTeSR1培養基(STEMCELL Technologies公司)一起培養。將細胞在含有10% CO_2的37°C培養箱中培養。hiPSCs細胞株的特徵在於典型的誘導性多能幹細胞(iPSCs)形態以及鹼性磷酸酶活性呈現陽性，RT-PCR以及西方墨點分析證實典型多能性標記物的表現。

【0051】 1.5 細胞活性分析

【0052】 將誘導性多能幹細胞(iPSCs)以每孔5 x 10^4個細胞的濃度接種到96孔盤中。培養24小時後，加入與BSA混合的不同劑量的cND-mC-C/C9並培養2天。將10 μl細胞計數測定套組8溶液(CCK-8，Sigma公司)添加至每個孔中，並作用2小時。在微量盤分析儀上測量490 nm處的吸光度。以10μl StemFlex培養基(Thermo

Fisher Scientific公司)代替CCK-8溶液處理的細胞作為陰性對照。所有實驗均獨立進行三次。

【0053】 1.6 動物

【0054】 C57BL/6雄性小鼠(6~10週齡)購自國家實驗動物中心(台北，台灣)。老鼠被飼養在無病原體的地方，並根據國家研究委員會的*實驗動物之護理暨使用指南*進行操作。所有麻醉及處死程序均經過台北榮民總醫院(Taipei Veterans General Hospital，TVGH)動物保護暨使用委員會的審查及批准。透過腹膜內注射以250 mg/kg三溴乙醇(Sigma-Aldrich公司)麻醉小鼠，並置於解剖顯微鏡(SZX16，OLYMPUS公司，日本)或光譜域OCT影像系統下。

【0055】 1.7. 玻璃體內注射

【0056】 對每隻小鼠玻璃體內注射5 μl不同的奈米鑽石粒子製劑至兩隻眼睛中。單側施用負載有*Cas9-GFP* (15 ng/μl)以及*Rs1-sgRNA* (30 ng/μl)構築體的奈米鑽石粒子混合物，負載*Cas9-GFP* (15 ng/μl)的奈米鑽石粒子對側眼為對照。使用漢彌頓注射器將5 μl的奈米鑽石粒子透過小鼠角膜緣後的鞏膜注射至眼睛的玻璃體腔中。在該過程中，約5 μl玻璃體液透過穿刺孔流出，以完全傳輸5 μl奈米鑽石粒子製劑。

【0057】 1.8. 光譜域OCT影像

【0058】 如前所述[33]，使用連續、高速、高解析度的視網膜影像採集系統(軸向解析度為7 μm；採集速度為76幀/秒，在XZ平面上為1000 x 1024像素)獲得小鼠視網膜的OCT影像。透過眼底獲得400幅影像的水平掃描。

【0059】 1.9. 微滴式數位PCR (Droplet digital PCR，ddPCR)

【0060】 透過ddPCR (BioRad公司)定量基因組DNA複製數。所有引子及探針序列(補充表1)均在OligoAnalyzer軟體(IDT公司)上設計。在液滴中使用探針的ddPCR Supermix (無dUTP)。

【0061】 1.10 統計分析

【0062】 未配對學生氏t檢驗用於評估數值數據的統計顯著性。統計顯著性設定為p值小於0.05。使用Excel軟體進行計算。

【0063】 2. 結果

【0064】 2.1 設計CRISPR-Cas9構築體以引入*RS1*突變及mCherry標記的奈米鑽石粒子的功能化以進行傳遞

【0065】 於本研究中，我們的目標在於開發透過使用奈米鑽石粒子以創造X染色體串聯視網膜裂損症(XLRS)疾病模型之方法，藉由將奈米鑽石粒子作為CRISPR-Cas9基因組編輯系統的載體，以修飾X染色體串聯視網膜裂損症(XLRS)相關的*RS1*基因。*RS1*突變c.625> T導致胺基酸取代p.R209C，為X染色體串聯視網膜裂損症(XLRS)中已知的致病突變之一。攜帶這種突變的患者(圖1A)的特徵為X染色體串聯視網膜裂損症(XLRS)的典型特徵，例如，透過眼底鏡檢查鏡觀察到的視網膜明顯發展為雙側黃斑萎縮(圖1B)，以及透過光學同調斷層掃描(optical coherence tomography，OCT)觀察到的兩隻眼睛都有的典型的分裂性表型(圖1C)。為了表現CRISPR-Cas9編輯系統的組份，設計了兩個線性DNA構築體。*RS1-sgRNA*構築體包含一個同源性定向修復(homology directed repair，HDR)模板，並編碼指導*RS1*基因第6外顯子中c.625> T突變的sgRNA (圖2A)。*Cas9-GFP*構築體編碼Cas9核酸內切酶以及GFP報導基因(圖2A)。

【0066】 原始奈米鑽石粒子透過爆轟法獲得，其直徑為3 nm。為了附著運送物，透過使用強氧化性酸引入羧基來官能化奈米鑽石粒子的表面。然後，羧化奈米鑽石粒子(cND)透過羧基與mCherry蛋白共價連接，進而可以螢光檢測這些顆粒(cND-mC)(圖2B及圖2C)。mCherry蛋白經設計可攜帶多聚組胺酸尾部，用於共價連接線性DNA的5'-磷酸基團，編碼CRISPR-Cas9編輯系統的組分(圖2B)。透過瓊脂糖凝膠電泳分析，我們顯示DNA與cND-mC顆粒結合(圖2D)。透過比較cND、cND-mC，以及cND-mC-C/C9奈米粒子的傅立葉轉換紅外(FTIR)光譜，我們發現在後兩種類型中觀察到1640 cm^{-1}處的獨特FTIR峰，表示mCherry蛋白的存在(圖2E)。同時，在cND-mC-C/C9奈米粒子的FTIR光譜中觀察到指示DNA部分存在的峰(圖2D)。將所得的攜帶mCherry以及CRISPR-Cas9編碼線性DNA (cND-mC-C/C9)的奈米鑽石粒子與牛血清白蛋白(BSA)混合以促進其向細胞的傳輸，並透過穿透式電子顯微鏡(TEM)觀察其平均值，由ImageJ確定的尺寸為5.6 +/- 0.99 nm (圖2F)。

【0067】 2.2 在hiPSCs中透過cND-mC-C/C9編輯*RS1*基因

【0068】 作為我們的最初目標，我們的目的在於使用cND-mC-C/C9奈米粒子在人類誘導性多能幹細胞(hiPSCs)中引入X染色體串聯視網膜裂損症(XLRS)相關的*RS1*突變。先前的研究顯示，BSA可穩定螢光亮度並防止奈米鑽石粒子在磷酸鹽緩衝液中聚集[34, 35]。因此，我們以在PBS中稀釋的cND-mC-C/C9顆粒以不同濃度的BSA (0%、1%，以及3%)處理了hiPSCs培養物。為了評估hiPSCs是否將cND-mC-C/C9奈米顆粒內化，在螢光顯微鏡下觀察了螢光標記的表現。在細胞內觀察到來自mCherry及GFP的螢光訊號，這表示cND-mC-C/C9顆粒均被內化且附著的DNA被轉錄(圖3A)。在以3%BSA cND-mC-C/C9處理的細胞內，mCherry

螢光點的平均大小明顯較小，表示與BSA混合可防止顆粒聚集(圖3B)。此外，相較於不含BSA以及與1% BSA混合的奈米顆粒，與3% BSA混合的cND-mC-C/C9更有效地傳輸到細胞中(圖3C)。以混合3% BSA的cND-mC-C/C9處理hiPSCs後兩天，透過流式細胞儀分選表現GFP的細胞。透過微滴式數位PCR (ddPCR)分析基因組DNA中的*RS1* c.625> T基因突變，結果顯示該核苷酸在所有等位基因的約19.3%中被編輯(圖3D)。為了測試cND-mC-C/C9是否具有任何毒性作用，以不同濃度的3% BSA混合的cND-mC-C/C9奈米顆粒處理hiPSCs兩天，並透過CCK-8分析評估其生存能力。結果顯示，在1.5至24 μg/ml的濃度範圍內，cND-mC-C/C9不會影響hiPSCs的活力(圖3E)。總而言之，這些結果顯示，混有BSA的cND-mC-C/C9奈米顆粒可被傳輸至hiPSCs，成功編輯其基因組，且不影響其生存能力。

【0069】 2.3 將cND-mC-C/C9傳輸到小鼠視網膜中

【0070】 為了研究cND-mC-C/C9在體內的作用，我們檢查cND-mC-C/C9輸注後奈米顆粒在小鼠視網膜中的分佈。透過玻璃體內注射將cND-mC-C/C9顆粒與3% BSA混合後注入小鼠眼內，並在兩週的時間內對動物進行掃描雷射光眼底鏡檢查(scanning laser ophthalmoscopy, SLO)。在視網膜的眼底清楚地觀察到GFP的螢光訊號，表示cND-mC-C/C9的內化及表現(圖4A)。視網膜橫斷面的共聚焦顯微鏡檢查顯示在不同的視網膜層中存在mCherry訊號及GFP表現，包括光受體(photoreceptor, PR)、外核層(ONL)、內核層(INL)，以及視網膜神經節細胞(RGC)層(圖4B及圖4C)。此外，視網膜橫斷面的H&E染色顯示cND-mC-C/C9輸注不影響視網膜結構(圖4D)。這些發現顯示，將cND-mC-C/C9與BSA混合可代表一種安全有效的視網膜傳輸系統。

【0071】 2.4 cND-mC-C/C9在小鼠視網膜中對*Rs1*基因的編輯

【0072】我們試圖研究透過cND-mC-C/C9奈米粒子在小鼠視網膜中進行基因組編輯的效率及功能效果。設計兩個線性DNA構築體：編碼sgRNA並包含HDR模板插入片段的*Rs1-sgRNA*，以及編碼Cas9核酸內切酶與GFP報導基因的*Cas9-GFP*，將c.625C> T突變引入小鼠*Rs1*基因中(圖5A)。將這些構築體附著到cND-mC奈米顆粒上以產生cND-mC-C/C9，然後將其注入小鼠眼中。注射後兩週，透過ddPCR評估視網膜裂解物中編輯的等位基因的百分比，發現其比注射僅帶有*Cas9-GFP*構築體的cND-mC-C/C9顆粒的小鼠視網膜中檢測到的背景訊號高約四倍(圖5B)。透過高解析度OCT觀察這些視網膜的精細解剖結構[36]。儘管以攜帶*Cas9-GFP*構築體的cND-mC-C/C9處理的視網膜僅顯示正常組織的層狀結構，但以兩種構築體處理的視網膜的特徵為高反射性外部視網膜帶2及3之間的高度不確定邊界，對應於橢球區域分別為光受體內層部分(IS)以及光受體外層部分(OS)的吞噬區(圖5C)。在經Cas9 + sgRNA處理的視網膜中，組合的超反射性外部視網膜帶2及3的厚度顯著降低約30% (圖5D)。同樣地，組織學切片的H&E染色也顯示內層部分(IS)/外層部分(OS)層的厚度減小(圖5E及圖5F)。此外，組織學切片顯示出鬆散的外核層(ONL)及內核層(INL)結構，這從OCT影像中並不明顯(圖5E)。綜上所述，我們的發現顯示cND-mC-C/C9處理會導致感光層(外核層(ONL)、內層部分(IS)以及外層部分(OS))的組織破壞。

【0073】2.5 cND-mC-C/C9媒介*Rs1*編輯對小鼠視網膜光受體細胞之影響

【0074】為了進一步研究cND媒介*Rs1*基因編輯對光受體的影響，我們在小鼠視網膜的橫截面中免疫染色光受體標記，例如視紫紅質、視錐細胞特異性視蛋白、恢復素，以及RS1。RS1蛋白通常在小鼠視網膜的光受體細胞及雙極細胞中表現[13]。於本文中，我們觀察到在對照視網膜中(以僅攜帶*Cas9-GFP*的cND-mC-

C/C9處理)，RS1蛋白富集在光受體的內層部分(IS)層中，但其定位也擴展到了外核層(ONL)、外網狀層(OPL)，以及內核層(INL)(圖6A，中)。另一方面，以攜帶兩種CRISPR-Cas9構築體的cND-mC-C/C9顆粒處理的視網膜的特徵為在IS層中的定位更加集中，而在其他層的擴散則更少(圖6A，中)。錐體細胞特異性視蛋白通常位於錐體細胞的外部，並在免疫螢光染色影像中以線性且平行訊號的形式出現[37]。實際上，在以對照cND-mC-C/C9(僅Cas9)處理的視網膜中觀察到視錐細胞特異性視蛋白的這種定位模式。相反地，以*Rs1*為目標的cND-mC-C/C9處理的視網膜的特徵在於視蛋白訊號明顯更短且呈點狀出現(圖6A及圖6C)。回收蛋白已知在桿狀、錐狀，以及雙極細胞中表現，而視紫紅質被認為是桿狀細胞的標記物[38-40]。免疫螢光染色的結果顯示，恢復素在對照小鼠視網膜的外網狀層(OPL)、外核層(ONL)、內層部分(IS)，以及外層部分(OS)中具有顯著的免疫反應性(圖6B，左)。此外，視紫紅質在外層部分(OS)中具有很強的免疫反應性(圖6B，中)。注射以*Rs1*為目標的cND-mC-C/C9 (Cas9 + sgRNA)明顯導致內層部分(IS)/外層部分(OS)區域中恢復素與視紫紅質的定位更加混亂，此外，外網狀層(OPL)中恢復素的存在也是不規則的(圖6B，左)。

【0075】 總之，基於奈米鑽石粒子的傳輸系統目的在於將CRISPR-Cas9組分傳輸至人類iPSCs以及小鼠視網膜中。為此，透過添加羧基官能化奈米鑽石粒子，羧基用於連接mCherry蛋白並共價連接CRISPR-Cas9系統的線性DNA編碼組份，包括HDR模板、sgRNA、Cas9蛋白，以及GFP報導基因。這些奈米鑽石粒子可被iPSCs以及小鼠視網膜內化，並可引入*RS1*基因的X染色體串聯視網膜裂損症(XLRS)特異性突變。奈米鑽石粒子與BSA的混合顯著增加細胞的攝取。我們證明裝載CRISPR-Cas9的奈米鑽石粒子處理小鼠視網膜會導致光受體細胞組織缺

陷，這是X染色體串聯視網膜裂損症(XLRS)的典型特徵。因此，我們認為我們基於奈米鑽石粒子的基因組編輯策略在建立X染色體串聯視網膜裂損症(XLRS)的體內及體外疾病模型方面具有極大的潛力(圖7)。

【0076】 儘管本說明書包含許多細節，但是這些細節不應被解釋為對本發明之範圍或可要求保護的範圍之限制，而是對特定實施例或本發明示例的特徵之描述。於本說明書中在單獨的實施例或示例的上下文中描述的某些特徵也可以在單個實施例中組合實現。

參考文獻

[1] S.K. Sikkink, S. Biswas, N.R. Parry, P.E. Stanga, D. Trump, X-linked retinoschisis: an update, J Med Genet 44(4) (2007) 225-32.

[2] R.S. Molday, U. Kellner, B.H. Weber, X-linked juvenile retinoschisis: clinical diagnosis, genetic analysis, and molecular mechanisms, Prog Retin Eye Res 31(3) (2012) 195-212.

[3] A. Tantri, T.R. Vrabec, A. Cu-Unjieng, A. Frost, W.H. Annesley, Jr., L.A. Donoso, X-linked retinoschisis: a clinical and molecular genetic review, Surv Ophthalmol 49(2) (2004) 214-30.

[4] C.G. Sauer, A. Gehrig, R. Warneke-Wittstock, A. Marquardt, C.C. Ewing, A. Gibson, B. Lorenz, B. Jurklies, B.H. Weber, Positional cloning of the gene associated with X-linked juvenile retinoschisis, Nature genetics 17(2) (1997) 164-70.

[5] W.W. Wu, R.S. Molday, Defective discoidin domain structure, subunit assembly, and endoplasmic reticulum processing of retinoschisin are primary mechanisms responsible for X-linked retinoschisis, J Biol Chem 278(30) (2003) 28139-46.

[6] C.A. Curat, M. Eck, X. Dervillez, W.F. Vogel, Mapping of epitopes in discoidin domain receptor 1 critical for collagen binding, J Biol Chem 276(49) (2001) 45952-8.

[7] W. Vogel, Discoidin domain receptors: structural relations and functional implications, FASEB journal : official publication of the Federation of American Societies for Experimental Biology 13 Suppl (1999) S77-82.

[8] L.C. Eksandh, V. Ponjavic, R. Ayyagari, E.L. Bingham, K.T. Hiriyanna, S. Andreasson, B. Ehinger, P.A. Sieving, Phenotypic expression of juvenile X-linked retinoschisis in Swedish families with different mutations in the XLRS1 gene, Archives of ophthalmology (Chicago, Ill. : 1960) 118(8) (2000) 1098-104.

[9] Y. Inoue, S. Yamamoto, M. Okada, M. Tsujikawa, T. Inoue, A.A. Okada, S. Kusaka, Y. Saito, K. Wakabayashi, Y. Miyake, T. Fujikado, Y. Tano, X-linked retinoschisis with point mutations in the XLRS1 gene, Archives of ophthalmology (Chicago, Ill. : 1960) 118(1) (2000) 93-6.

[10] X. Li, X. Ma, Y. Tao, Clinical features of X linked juvenile retinoschisis in Chinese families associated with novel mutations in the RS1 gene, Molecular vision 13 (2007) 804-12.

[11] T. Wang, A. Zhou, C.T. Waters, E. O'Connor, R.J. Read, D. Trump, Molecular pathology of X linked retinoschisis: mutations interfere with retinoschisin secretion and oligomerisation, Br J Ophthalmol 90(1) (2006) 81-6.

[12] C.M. Mooy, L.I. Van Den Born, S. Baarsma, D.A. Paridaens, T. Kraaijenbrink, A. Bergen, B.H. Weber, Hereditary X-linked juvenile retinoschisis: a review of the role of Muller cells, Archives of ophthalmology (Chicago, Ill. : 1960) 120(7) (2002) 979-84.

[13] L.L. Molday, D. Hicks, C.G. Sauer, B.H. Weber, R.S. Molday, Expression of X-linked retinoschisis protein RS1 in photoreceptor and bipolar cells, Investigative ophthalmology & visual science 42(3) (2001) 816-25.

[14] S.N. Reid, C. Yamashita, D.B. Farber, Retinoschisin, a photoreceptor-secreted protein, and its interaction with bipolar and muller cells, The Journal of neuroscience : the official journal of the Society for Neuroscience 23(14) (2003) 6030-40.

[15] Z.Y. Lien, T.C. Hsu, K.K. Liu, W.S. Liao, K.C. Hwang, J.I. Chao, Cancer cell labeling and tracking using fluorescent and magnetic nanodiamond, Biomaterials 33(26) (2012) 6172-85.

[16] K.K. Liu, C.C. Wang, C.L. Cheng, J.I. Chao, Endocytic carboxylated nanodiamond for the labeling and tracking of cell division and differentiation in cancer and stem cells, Biomaterials 30(26) (2009) 4249-59.

[17] L. Moore, J. Yang, T.T. Lan, E. Osawa, D.K. Lee, W.D. Johnson, J. Xi, E.K. Chow, D. Ho, Biocompatibility Assessment of Detonation Nanodiamond in Non-Human Primates and Rats Using Histological, Hematologic, and Urine Analysis, ACS Nano 10(8) (2016) 7385-400.

[18] C.C. Fu, H.Y. Lee, K. Chen, T.S. Lim, H.Y. Wu, P.K. Lin, P.K. Wei, P.H. Tsao, H.C. Chang, W. Fann, Characterization and application of single fluorescent nanodiamonds as cellular biomarkers, Proceedings of the National Academy of Sciences of the United States of America 104(3) (2007) 727-32.

[19] X.Q. Zhang, M. Chen, R. Lam, X. Xu, E. Osawa, D. Ho, Polymer-functionalized nanodiamond platforms as vehicles for gene delivery, ACS Nano 3(9) (2009) 2609-16.

[20] H.L. Chu, H.W. Chen, S.H. Tseng, M.H. Hsu, L.P. Ho, F.H. Chou, M.P. Li, Y.C. Chang, P.H. Chen, L.Y. Tsai, C.C. Chou, J.S. Chen, T.M. Cheng, C.C. Chang,

Development of a growth-hormone-conjugated nanodiamond complex for cancer therapy, ChemMedChem 9(5) (2014) 1023-9.

[21] C.Y. Cheng, E. Perevedentseva, J.S. Tu, P.H. Chung, C.L. Cheng, K.K. Liu, J.I. Chao, P.H. Chen, C.C. Chang, Direct and in vitro observation of growth hormone receptor molecules in A549 human lung epithelial cells by nanodiamond labeling, Applied Physics Letters 90(16) (2007).

[22] M.G. Chernysheva, I.Y. Myasnikov, G.A. Badun, Myramistin adsorption on detonation nanodiamonds in the development of drug delivery platforms, Diamond and Related Materials 55 (2015) 45-51.

[23] V.N. Mochalin, A. Pentecost, X.M. Li, I. Neitzel, M. Nelson, C. Wei, T. He, F. Guo, Y. Gogotsi, Adsorption of drugs on nanodiamond: toward development of a drug delivery platform, Mol Pharm 10(10) (2013) 3728-35.

[24] K. Turcheniuk, V.N. Mochalin, Biomedical applications of nanodiamond (Review), Nanotechnology 28(25) (2017) 252001.

[25] H.S. Choi, W. Liu, P. Misra, E. Tanaka, J.P. Zimmer, B. Itty Ipe, M.G. Bawendi, J.V. Frangioni, Renal clearance of quantum dots, Nat Biotechnol 25(10) (2007) 1165-70.

[26] Z.U. Hasan, P.R. Hemmer, H. Lee, A.L. Migdall, O. Shenderova, N. Nunn, T. Oeckinghaus, M. Torelli, G. McGuire, K. Smith, E. Danilov, R. Reuter, J. Wrachtrup, A. Shames, D. Filonova, A. Kinev, Commercial quantities of ultrasmall fluorescent nanodiamonds containing color centers, Advances in Photonics of Quantum Computing, Memory, and Communication X, 2017.

[27] F.C. Barone, C. Marcinkiewicz, J. Li, M. Sternberg, P.I. Lelkes, D.A. Dikin, P.J. Bergold, J.A. Gerstenhaber, G. Feuerstein, Pilot study on biocompatibility of

fluorescent nanodiamond-(NV)-Z~800 particles in rats: safety, pharmacokinetics, and bio-distribution (part III), Int J Nanomedicine 13 (2018) 5449-5468.

[28] K. Purtov, A. Petunin, E. Inzhevatkin, A. Burov, N. Ronzhin, A. Puzyr, V. Bondar, Biodistribution of Different Sized Nanodiamonds in Mice, Journal of Nanoscience and Nanotechnology 15(2) (2015) 1070-1075.

[29] E. Perevedentseva, Y.C. Lin, M. Jani, C.L. Cheng, Biomedical applications of nanodiamonds in imaging and therapy, Nanomedicine (Lond) 8(12) (2013) 2041-60.

[30] M. Yu, J. Zheng, Clearance Pathways and Tumor Targeting of Imaging Nanoparticles, ACS Nano 9(7) (2015) 6655-74.

[31] E.R. Burnight, M. Gupta, L.A. Wiley, K.R. Anfinson, A. Tran, R. Triboulet, J.M. Hoffmann, D.L. Klaahsen, J.L. Andorf, C. Jiao, E.H. Sohn, M.K. Adur, J.W. Ross, R.F. Mullins, G.Q. Daley, T.M. Schlaeger, E.M. Stone, B.A. Tucker, Using CRISPR-Cas9 to Generate Gene-Corrected Autologous iPSCs for the Treatment of Inherited Retinal Degeneration, Mol Ther 25(9) (2017) 1999-2013.

[32] J.H. Chuang, A.A. Yarmishyn, D.K. Hwang, C.C. Hsu, M.L. Wang, Y.P. Yang, K.H. Chien, S.H. Chiou, C.H. Peng, S.J. Chen, Expression profiling of cell-intrinsic regulators in the process of differentiation of human iPSCs into retinal lineages, Stem Cell Res Ther 9(1) (2018) 140.

[33] P.H. Chen, C.H. Wu, Y.F. Chen, Y.C. Yeh, B.H. Lin, K.W. Chang, P.Y. Lai, M.C. Hou, C.L. Lu, W.C. Kuo, Combination of structural and vascular optical coherence tomography for differentiating oral lesions of mice in different carcinogenesis stages, Biomed Opt Express 9(4) (2018) 1461-1476.

[34] Y.K. Tzeng, O. Faklaris, B.M. Chang, Y. Kuo, J.H. Hsu, H.C. Chang, Superresolution imaging of albumin-conjugated fluorescent nanodiamonds in cells by stimulated emission depletion, Angew Chem Int Ed Engl 50(10) (2011) 2262-5.

[35] K.-i. Hanaki, A. Momo, T. Oku, A. Komoto, S. Maenosono, Y. Yamaguchi, K. Yamamoto, Semiconductor quantum dot/albumin complex is a long-life and highly photostable endosome marker, Biochemical and Biophysical Research Communications 302(3) (2003) 496-501.

[36] J.P. Syu, W. Buddhakosai, S.J. Chen, C.C. Ke, S.H. Chiou, W.C. Kuo, Supercontinuum source-based multi-contrast optical coherence tomography for rat retina imaging, Biomed Opt Express 9(12) (2018) 6132-6144.

[37] Y. Liang, D. Fotiadis, T. Maeda, A. Maeda, A. Modzelewska, S. Filipek, D.A. Saperstein, A. Engel, K. Palczewski, Rhodopsin signaling and organization in heterozygote rhodopsin knockout mice, J Biol Chem 279(46) (2004) 48189-96.

[38] A.H. Milam, D.M. Dacey, A.M. Dizhoor, Recoverin immunoreactivity in mammalian cone bipolar cells, Visual neuroscience 10(1) (1993) 1-12.

[39] K. Sakurai, J. Chen, S.C. Khani, V.J. Kefalov, Regulation of mammalian cone phototransduction by recoverin and rhodopsin kinase, J Biol Chem 290(14) (2015) 9239-50.

[40] K. Szabo, A. Szabo, A. Enzsoly, A. Szel, A. Lukats, Immunocytochemical analysis of misplaced rhodopsin-positive cells in the developing rodent retina, Cell and tissue research 356(1) (2014) 49-63.

【符號說明】無

【生物材料寄存】無

【序列表】

<110>

<120> 羧化奈米鑽石粒子媒介CRISPR-CAS9傳輸系統

<160> 4

<170> PatentIn version 3.5

<210> 1
<211> 96
<212> DNA
<213> 合成序列

<400> 1

GGCACGTCTG CATTGCCATC GTTTTAGAGC TAGAAATAGC AAGTTAAAAT AAGGCTAGTC 60

CGTTATCAAC TTGAAAAAGT GGCACCGAGT CGGTGC
96

<210> 2
<211> 190
<212> DNA
<213> 合成序列

<400> 2

GTCTTCTATG GCAACTCGGA CCGCACCTCC ACGGTTCAGA ACCTGCTGCG GCCCCCCATC 60

ATCTCCCGCT TCATCCGCCT CATCCCGCTG GGCTGGCATG TCCGGATTGC CATCCGGATG 120

GAGCTGCTGG AGTGCGTCAG CAAGTGTGCC TGATGCCTGC CTCAGCTCGG CGCCTGCCAG 180

GGGGTGACTG
190

<210> 3
<211> 96
<212> DNA
<213> 合成序列

<400> 3

GGCATGTCCG AATTGCCATC GTTTTAGAGC TAGAAATAGC AAGTTAAAAT AAGGCTAGTC 60

CGTTATCAAC TTGAAAAAGT GGCACCGAGT CGGTGC
96

<210> 4
<211> 190
<212> DNA
<213> 合成序列

<400> 4

GTCTTCTATG GAAACTCAGA CCGGAGTTCT ACAGTTCAGA ACTTACTCAG GCCCCCCATC 60

ATTTCCCGCT TCATCCGACT GATCCCTCTA GGCTGGCACG TCTGTATTGCC ATCCGGATGG 120

AGCTGCTTGA GTGTGCCAGC AAGTGTGCCT GATGTCTATT TCAGCTCAGT TCTGTCACTT 180

GCAGGGAGA 190

【發明申請專利範圍】

【請求項1】一種用於基因編輯的傳遞系統，包含奈米鑽石粒子(nanodiamond，ND)顆粒作為CRISPR-Cas9組分的載體，該CRISPR-Cas9組分包括一Cas9蛋白、一引導蛋白(gRNA)、一設計用於將一突變引入一給定基因以修復一組織損傷的模板DNA，其中該奈米鑽石粒子顆粒的直徑小於5 nm，且透過其表面的羧化作用而官能化並與一螢光蛋白共價結合；以及一用於表現該Cas9蛋白的第一線性DNA構築體以及一用於表現該gRNA/模板DNA的第二線性DNA構築體透過磷醯咪唑與該共價結合至該螢光蛋白的奈米鑽石粒子顆粒連接以獲得羧化奈米鑽石粒子媒介CRISPR- Cas9顆粒。

【請求項2】如請求項1所述之系統，其中該奈米鑽石粒子顆粒的直徑在3 nm-5 nm的範圍內。

【請求項3】如請求項1所述之系統，其中該奈米鑽石粒子顆粒的直徑為約3 nm。

【請求項4】如請求項1所述之系統，其中該螢光蛋白為mCherry蛋白。

【請求項5】如請求項1所述之系統，其中該顆粒在使用前以牛血清白蛋白(bovine serum albumin，BSA)包覆。

【請求項6】如請求項1所述之系統，其中該給定基因為與X染色體串聯視網膜裂損症(X-linked retinoschisis，XLRS)相關的*RS1*基因。

【請求項7】如請求項6所述之系統，其作為用於創造一X染色體串聯視網膜裂損症(XLRS)的體外及體內疾病模型之工具。

【請求項8】如請求項6所述之系統，其中該給定基因中的突變為經由兩個線性DNA構築體引入的，該線性DNA構築體與該結合的mCherry連接，且該第一線

性DNA構築體編碼Cas9核酸內切酶以及一綠色螢光蛋白(green fluorescent protein，GFP)報導基因，且該第二線性DNA構築體編碼一sgRNA，並包含一HDR模板的插入片段，該插入片段設計用於引入*RS1* c.625C> T突變。

【請求項9】 如請求項7所述之系統，其中該傳輸導致將*RS1* c.625C> T突變引入人類誘導性多能幹細胞(induced pluripotent stem cells，iPSCs)或小鼠視網膜中。

【請求項10】 一種如請求項1至9任一項所述之系統在治療一個體的一疾病或修復一組織損傷中之用途，包含透過如請求項1所述之系統將一給定基因中的突變傳輸並內化到該個體中。

【請求項11】 如請求項10所述之用途，其中該疾病為X染色體串聯視網膜裂損症(XLRS)。

【請求項12】 如請求項11所述之用途，其中該給定基因為與X染色體串聯視網膜裂損症(XLRS)相關的*RS1*基因。

【請求項13】 一種用於創造體外或體內疾病模型之方法，包含透過如請求項1所述之系統將一給定基因中的突變傳輸並內化到誘導性多能幹細胞(iPSCs)或一動物器官中。

【請求項14】 如請求項13所述之方法，其中該疾病為X染色體串聯視網膜裂損症(XLRS)。

【請求項15】 如請求項14所述之方法，其中該給定基因為與X染色體串聯視網膜裂損症(XLRS)相關的*RS1*基因。

【請求項16】 如請求項14所述之方法，其中該動物器官為小鼠視網膜。

【請求項17】 如請求項15所述之方法，其中該傳輸導致將*RS1* c.625C> T突變引入人類誘導性多能幹細胞(iPSCs)或小鼠視網膜。

【請求項18】 如請求項16所述之方法，其中在該小鼠視網膜中編輯的該*Rs1*基因導致幾種X染色體串聯視網膜裂損症(XLRS)典型的病理特徵。

【請求項19】 如請求項18所述之方法，其中該X染色體串聯視網膜裂損症(XLRS)典型的病理特徵為異常的光受體結構。

【發明圖式】

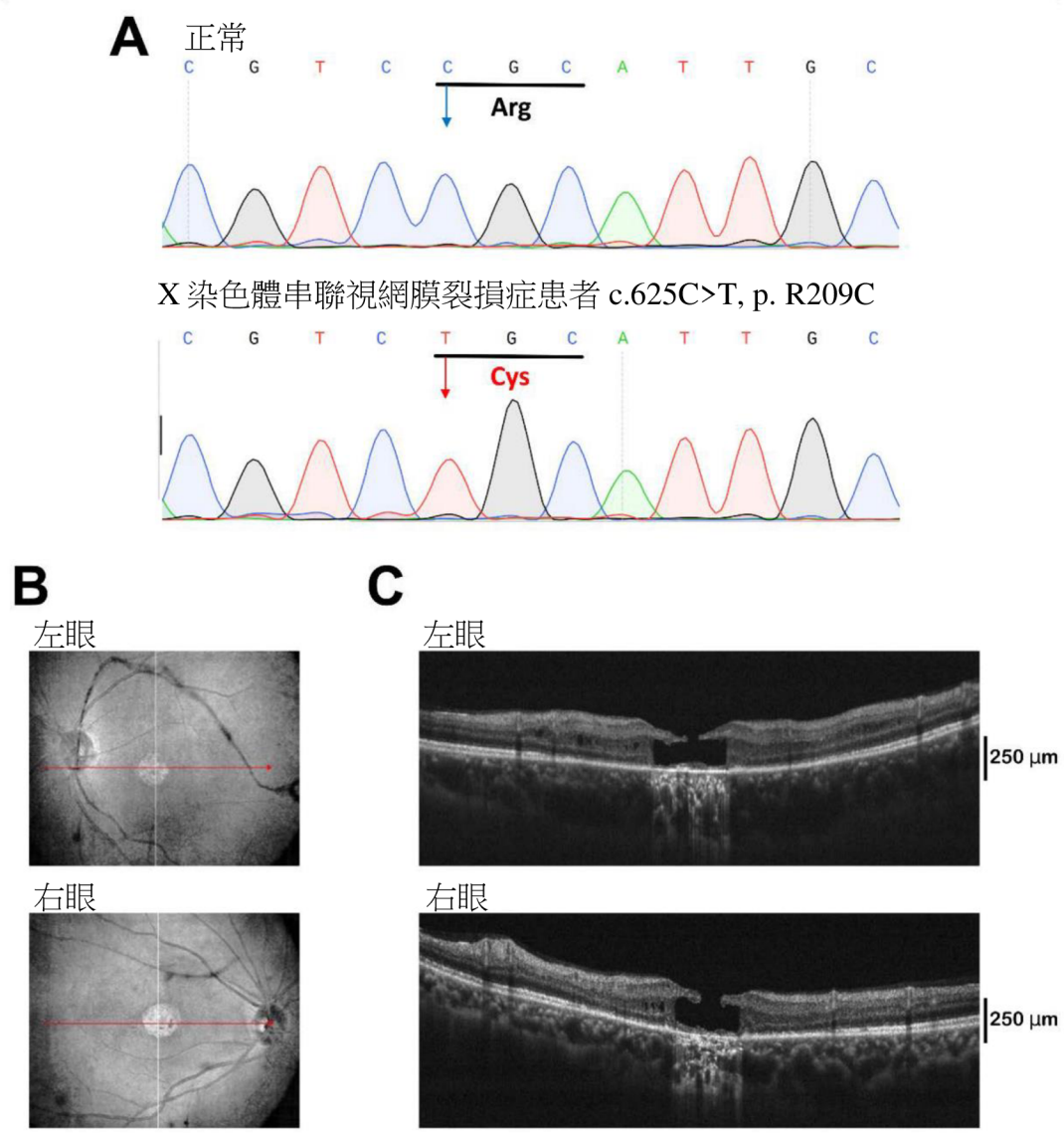
A
正常
C G T C C G C A T T G C
Arg
X 染色體串聯視網膜裂損症患者 c.625C>T, p. R209C
C G T C T G C A T T G C
Cys
B
左眼
右眼
C
左眼
右眼
250 µm
250 µm

【圖1】

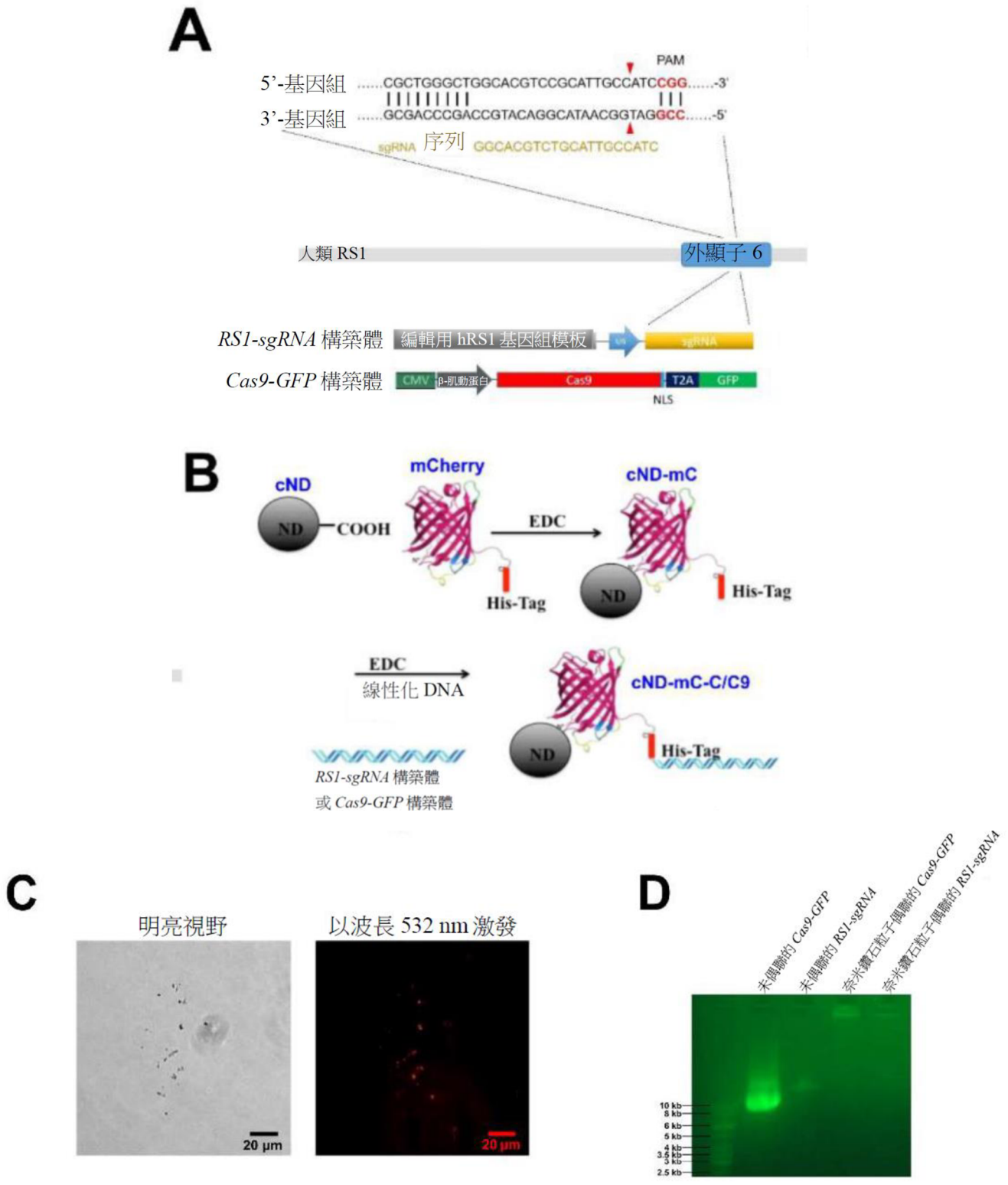
A
PAM
5'-基因組 .....CGCTGGGCTGGCACGTCCGCATTGCCATCCGG.....-3'
3'-基因組 .....GCGACCCGACCGTACAGGCATAACGGTAGGCC.....-5'
sgRNA 序列 GGCACGTCTGCATTGCCATC
人類 RS1
外顯子 6
RS1-sgRNA 構築體
編輯用 hRS1 基因組模板
sgRNA
Cas9-GFP 構築體
CMV
β-肌動蛋白
Cas9
T2A
GFP
NLS
B
cND
ND
COOH
mCherry
EDC
cND-mC
His-Tag
ND
His-Tag
EDC
線性化 DNA
cND-mC-C/C9
ND
His-Tag
RS1-sgRNA 構築體
或 Cas9-GFP 構築體
C
明亮視野
以波長 532 nm 激發
20 μm
20 μm
D
未偶聯的 Cas9-GFP
未偶聯的 RS1-sgRNA
奈米鑽石粒子偶聯的 Cas9-GFP
奈米鑽石粒子偶聯的 RS1-sgRNA
10 kb
8 kb
6 kb
5 kb
4 kb
3.5 kb
3 kb
2.5 kb

【圖2】

E

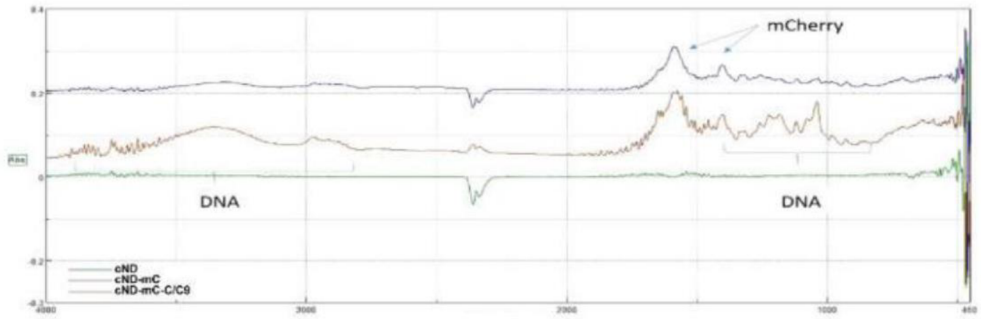

波長[cm^{-1}]

F

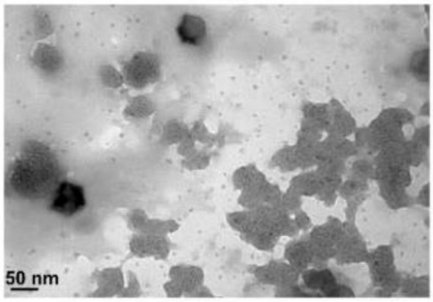

【圖2(續)】

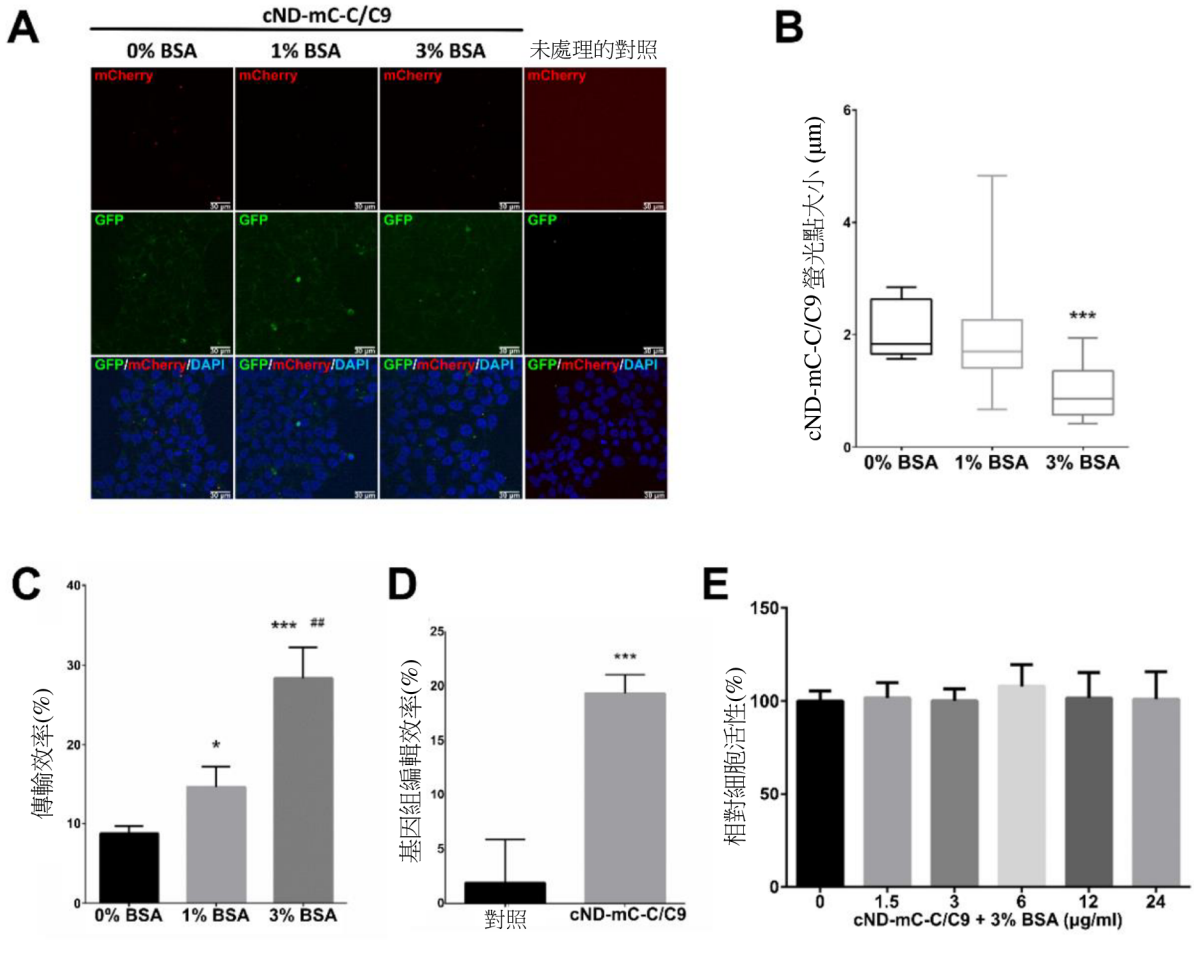
A
cND-mC-C/C9
0% BSA
1% BSA
3% BSA
未處理的對照
mCherry
GFP
GFP/mCherry/DAPI
B
cND-mC-C/C9 螢光點大小 (μm)
0% BSA
1% BSA
3% BSA
***
C
傳輸效率(%)
*
***
##
0% BSA
1% BSA
3% BSA
D
基因組編輯效率(%)
***
對照
cND-mC-C/C9
E
相對細胞活性(%)
0
1.5
3
6
12
24
cND-mC-C/C9 + 3% BSA (μg/ml)

【圖3】

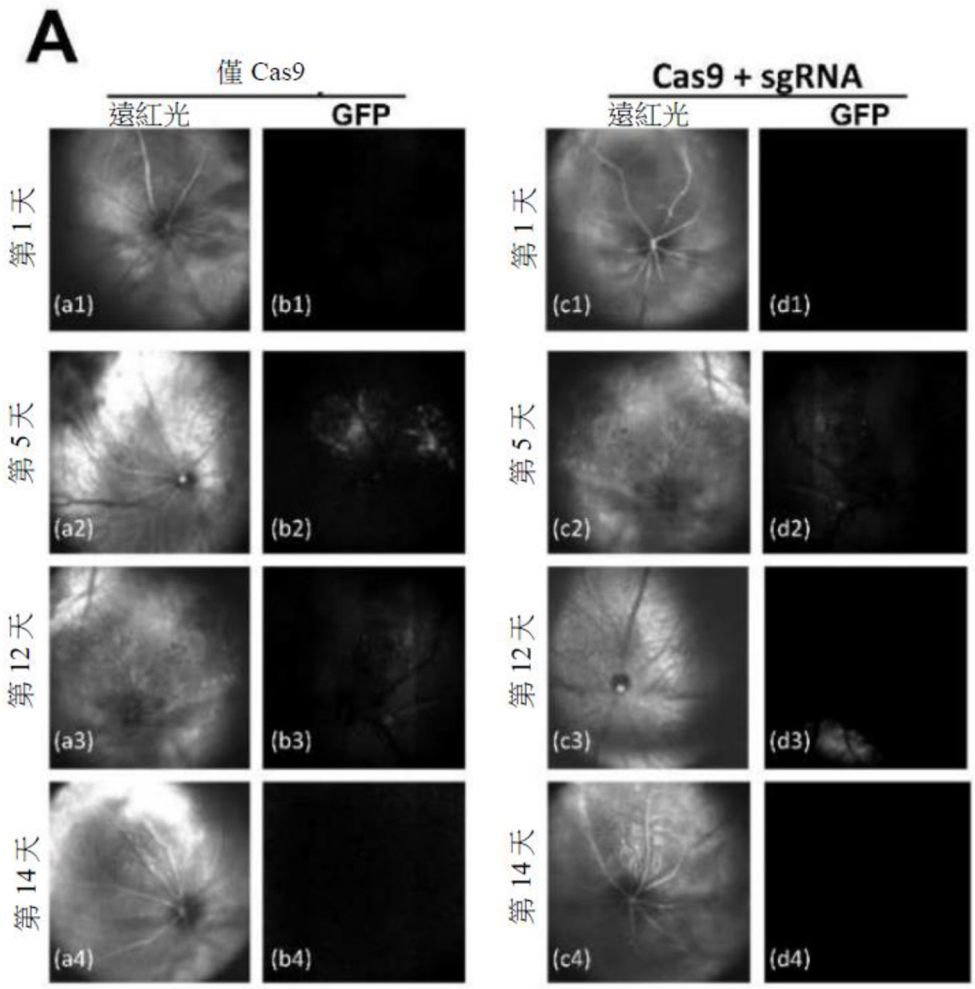
A
僅 Cas9
Cas9 + sgRNA
遠紅光
GFP
遠紅光
GFP
第 1 天
第 5 天
第 12 天
第 14 天
(a1)
(b1)
(c1)
(d1)
(a2)
(b2)
(c2)
(d2)
(a3)
(b3)
(c3)
(d3)
(a4)
(b4)
(c4)
(d4)

【圖4】

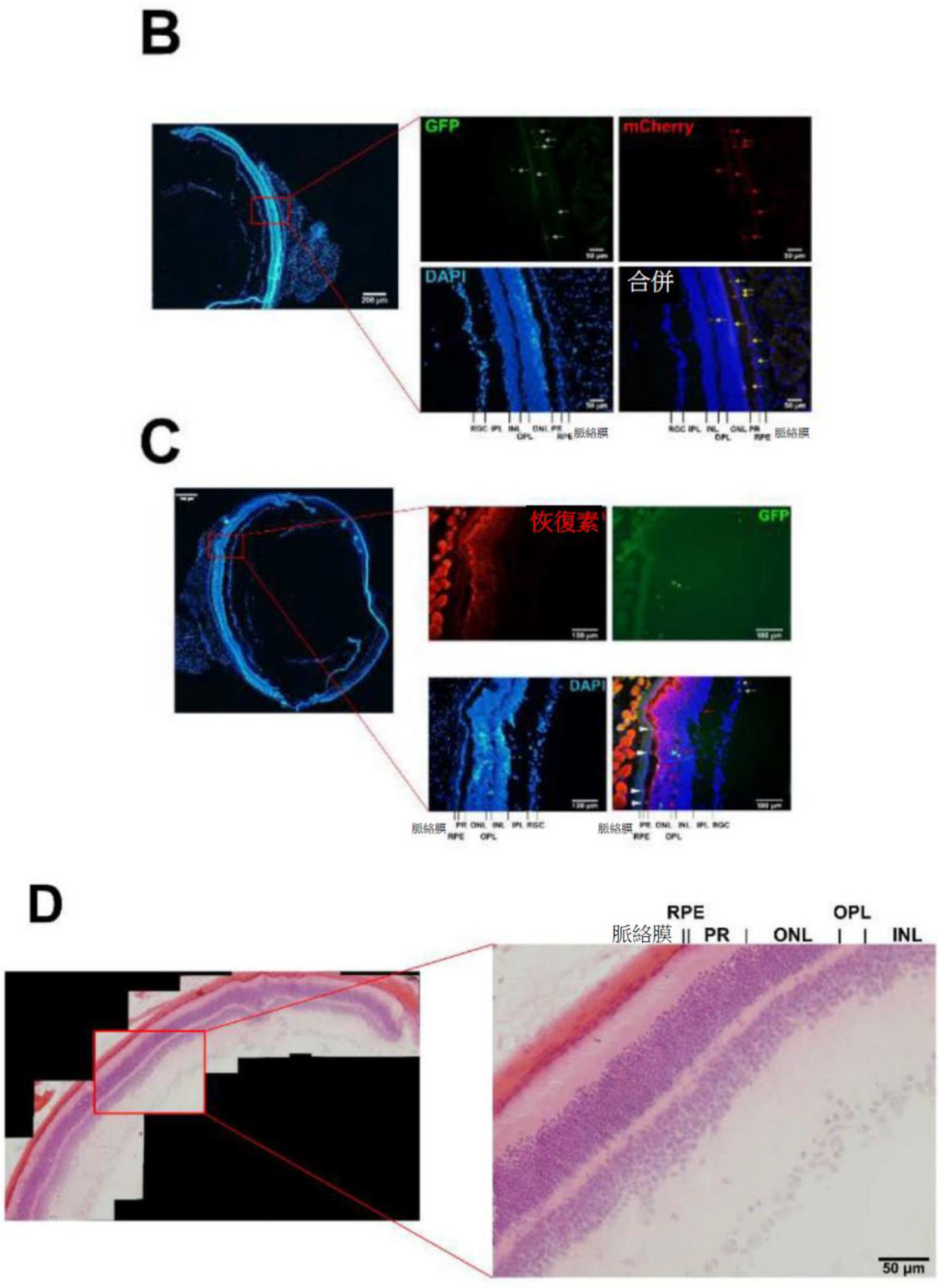
B
GFP
mCherry
DAPI
合併
RGC IPL INL OPL ONL PR RPE 脈絡膜
C
恢復素
GFP
DAPI
脈絡膜 PR ONL INL IPL RGC
RPE OPL
D
RPE
OPL
脈絡膜 PR ONL INL
50 μm

【圖4(續)】

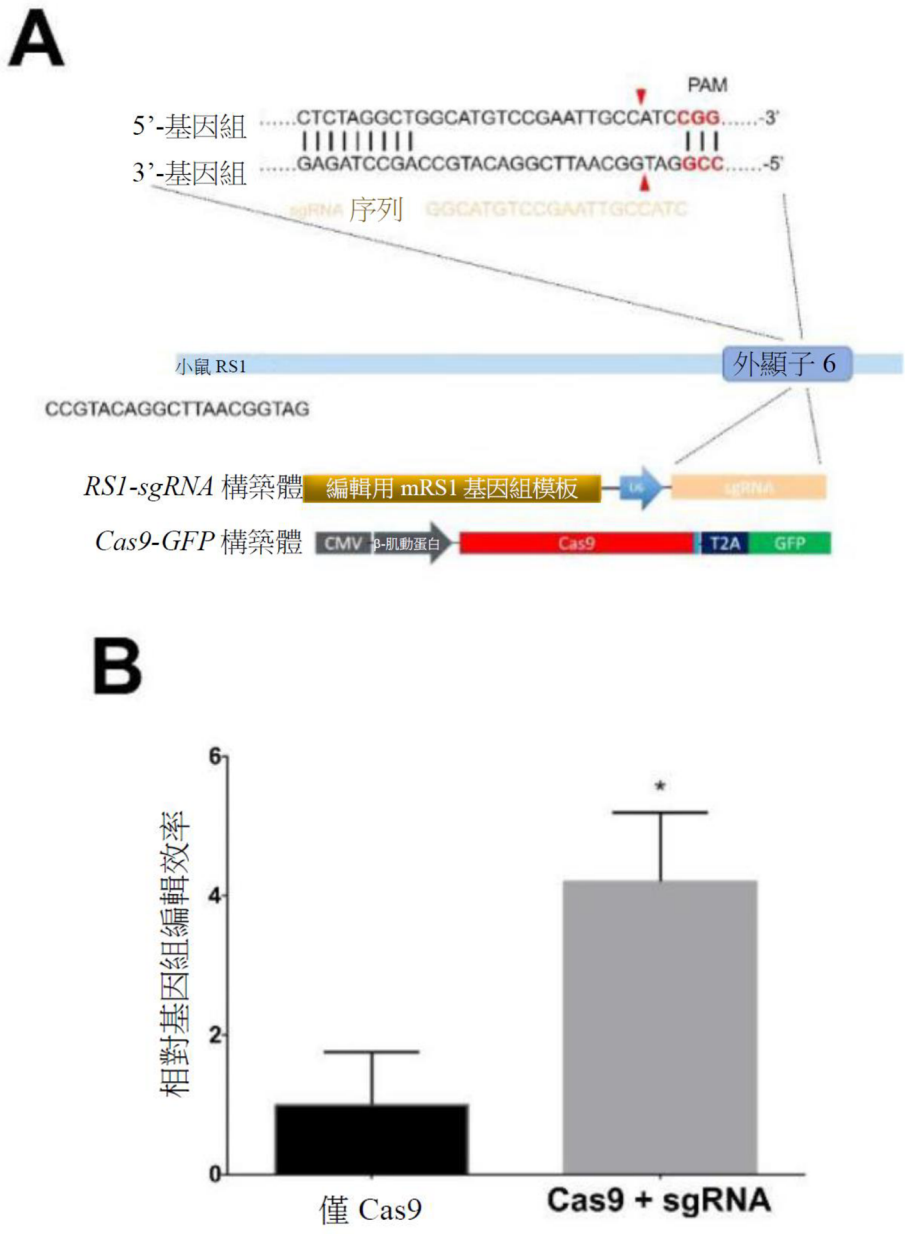
A
PAM
5'-基因組 .....CTCTAGGCTGGCATGTCCGAATTGCCATCCGG.....-3'
3'-基因組 .....GAGATCCGACCGTACAGGCTTAACGGTAGGCC.....-5'
sgRNA 序列 GGCATGTCCGAATTGCCATC
小鼠 RS1
外顯子 6
CCGTACAGGCTTAACGGTAG
RS1-sgRNA 構築體
編輯用 mRS1 基因組模板
U6
sgRNA
Cas9-GFP 構築體
CMV
β-肌動蛋白
Cas9
T2A
GFP
B
相對基因組編輯效率
6
4
2
0
*
僅 Cas9
Cas9 + sgRNA

【圖5】

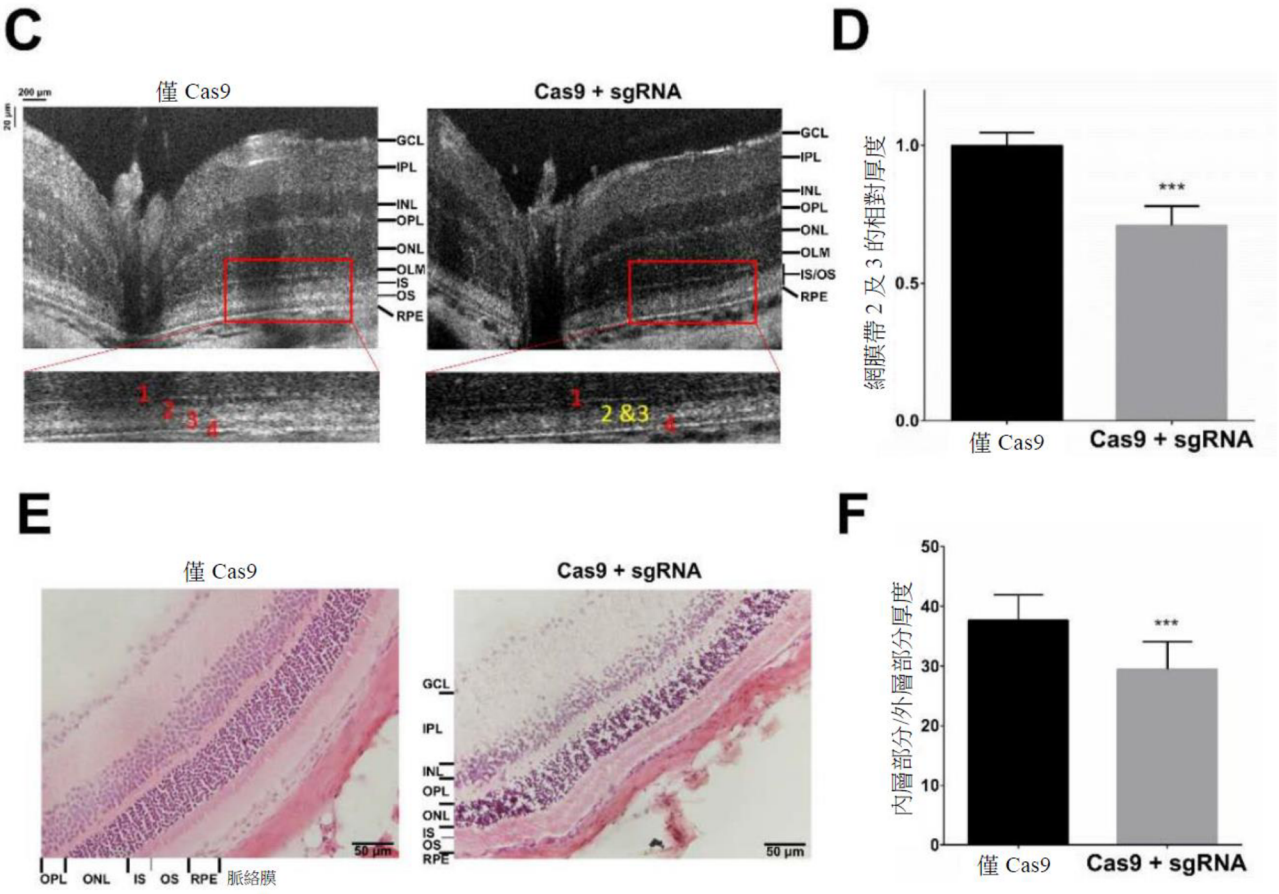
C
僅 Cas9
Cas9 + sgRNA
GCL
IPL
INL
OPL
ONL
OLM
IS
OS
IS/OS
RPE
1
2
3
4
2 &3
D
網膜帶 2 及 3 的相對厚度
1.0
0.5
0.0
***
僅 Cas9
Cas9 + sgRNA
E
僅 Cas9
Cas9 + sgRNA
50 μm
OPL
ONL
IS
OS
RPE
脈絡膜
F
內層部分/外層部分厚度
50
40
30
20
10
0
***
僅 Cas9
Cas9 + sgRNA

【圖5(續)】

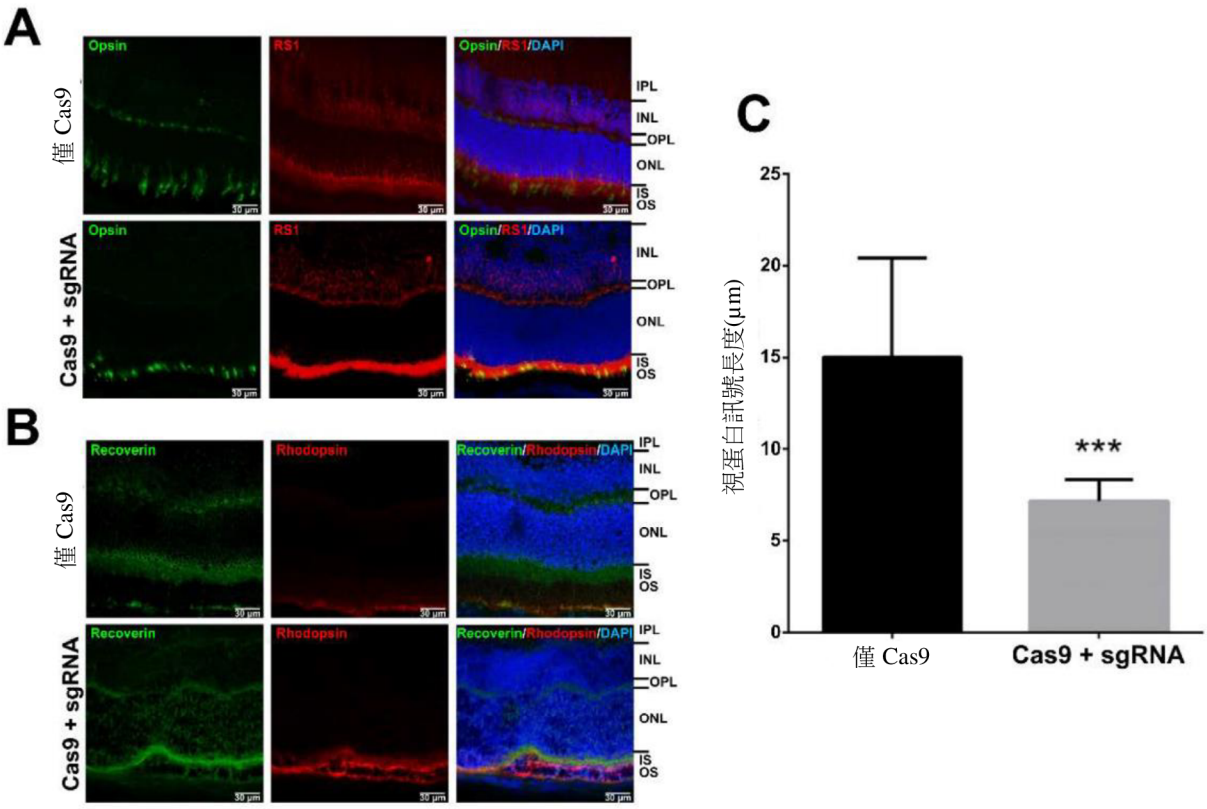
A
僅 Cas9
Cas9 + sgRNA
Opsin
RS1
Opsin/RS1/DAPI
IPL
INL
OPL
ONL
IS
OS
B
Recoverin
Rhodopsin
Recoverin/Rhodopsin/DAPI
C
視蛋白訊號長度(μm)
25
20
15
10
5
0
***
僅 Cas9
Cas9 + sgRNA

【圖6】

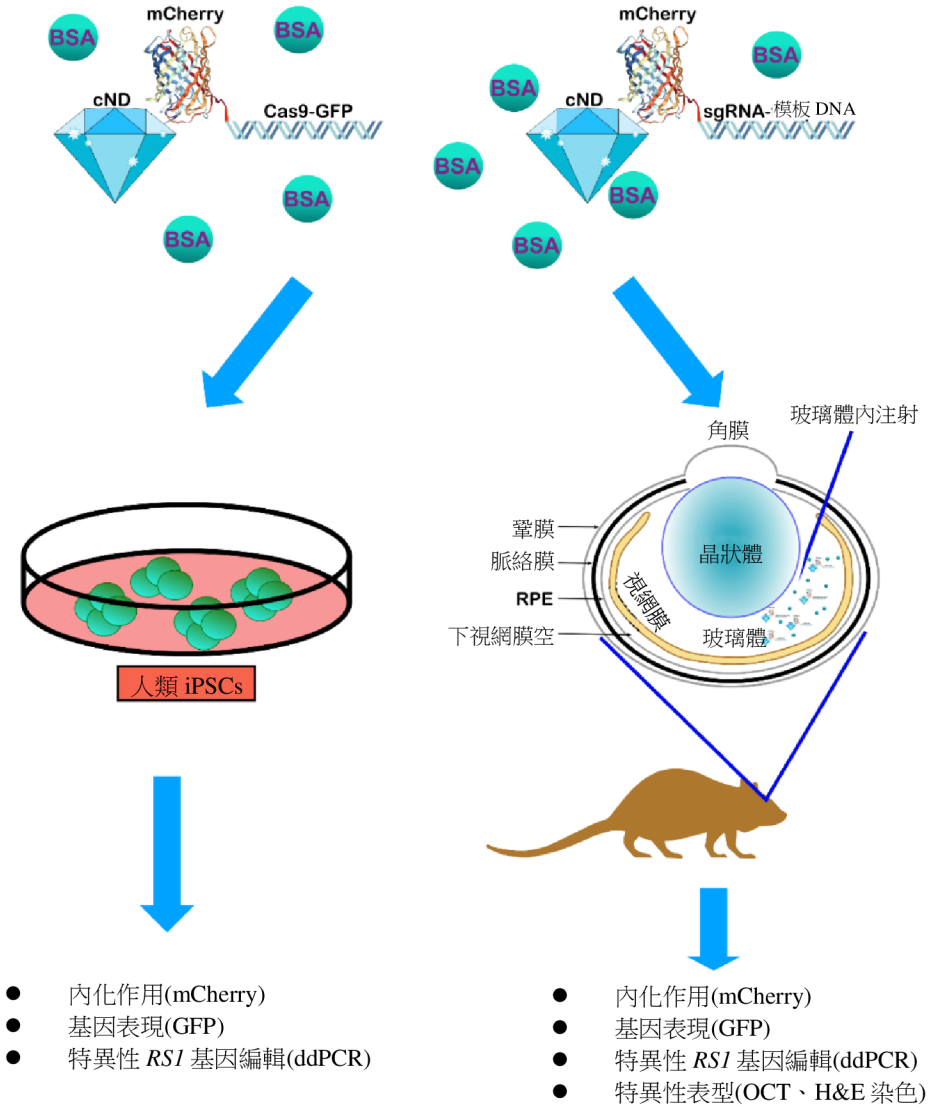
mCherry
BSA
cND
Cas9-GFP
sgRNA-模板 DNA
人類 iPSCs
角膜
玻璃體內注射
鞏膜
脈絡膜
RPE
下視網膜空
晶狀體
視網膜
玻璃體
內化作用(mCherry)
基因表現(GFP)
特異性 RS1 基因編輯(ddPCR)
內化作用(mCherry)
基因表現(GFP)
特異性 RS1 基因編輯(ddPCR)
特異性表型(OCT、H&E 染色)

【圖7】

US 20210108230A1

(19) **United States**

(12) **Patent Application Publication** (10) **Pub. No.: US 2021/0108230 A1**

CHIOU et al. (43) **Pub. Date: Apr. 15, 2021**

(54) **CARBOXYLATED NANODIAMOND-MEDIATED CRISPR-CAS9 DELIVERY SYSTEM**

(71) Applicants: **Taipei Veterans General Hospital**, Taipei City (TW); **National Chiao Tung University**, Hsinchu (TW); **National Cheng Kung University**, Tainan City (TW)

(72) Inventors: **Shih-Hwa CHIOU**, Taipei City (TW); **Tien-Chun YANG**, Taipei City (TW); **Chia-Ching CHANG**, Hsinchu City (TW); **Yon-Hua TZENG**, Tainan City (TW)

(73) Assignees: **Taipei Veterans General Hospital**, Taipei City (TW); **National Chiao Tung University**, Hsinchu (TW); **National Cheng Kung University**, Tainan City (TW)

(21) Appl. No.: **17/071,667**

(22) Filed: **Oct. 15, 2020**

Related U.S. Application Data

(60) Provisional application No. 62/915,143, filed on Oct. 15, 2019.

Publication Classification

(51) **Int. Cl.**

C12N 15/90	(2006.01)
A61K 9/51	(2006.01)
C12N 15/11	(2006.01)
C12N 9/22	(2006.01)

(52) **U.S. Cl.**

CPC ***C12N 15/907*** (2013.01); ***A61K 9/5115*** (2013.01); *C12N 2800/80* (2013.01); ***C12N 9/22*** (2013.01); *C12N 2310/20* (2017.05); ***C12N 15/11*** (2013.01)

(57) **ABSTRACT**

The present invention provides a carboxylated nanodiamond-mediated CRISPR-Cas**9** delivery system for gene editing comprising nanodiamond (ND) particles as the carriers of CRISPR-Cas**9** components designed to introduce the mutation in a given gene for repairing a tissue damage.

Specification includes a Sequence Listing.

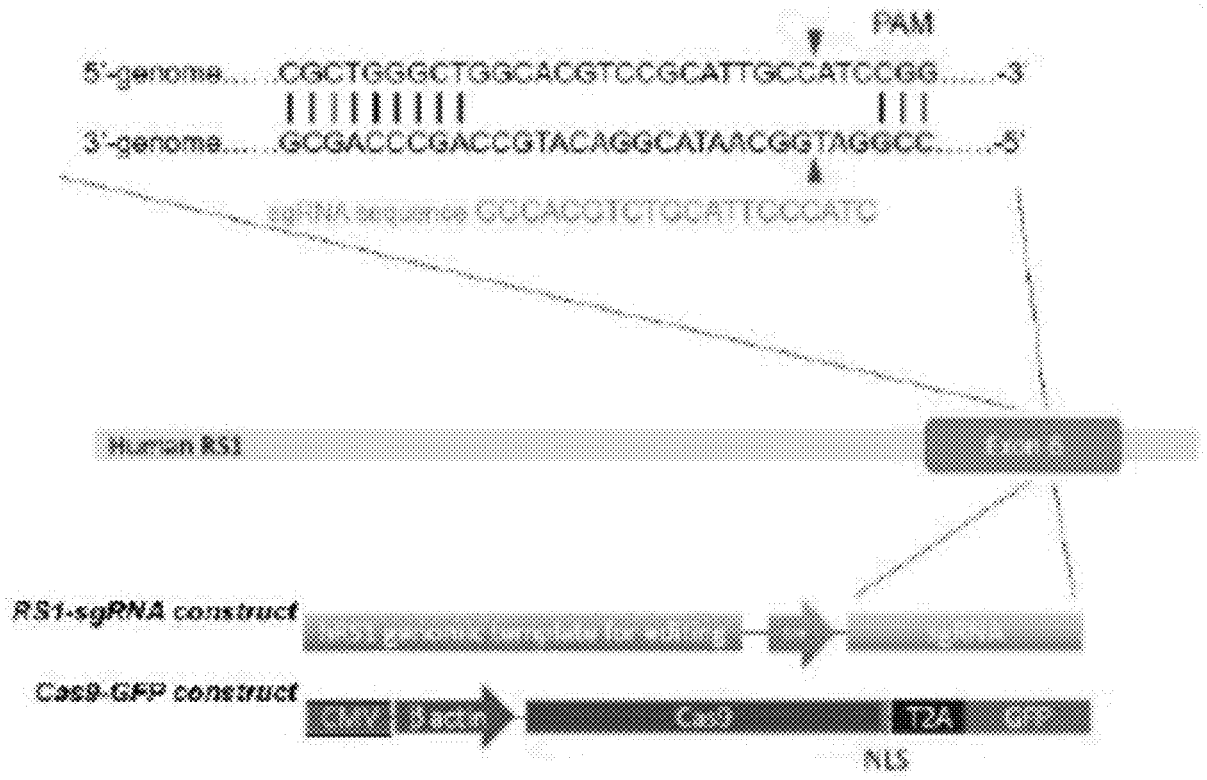

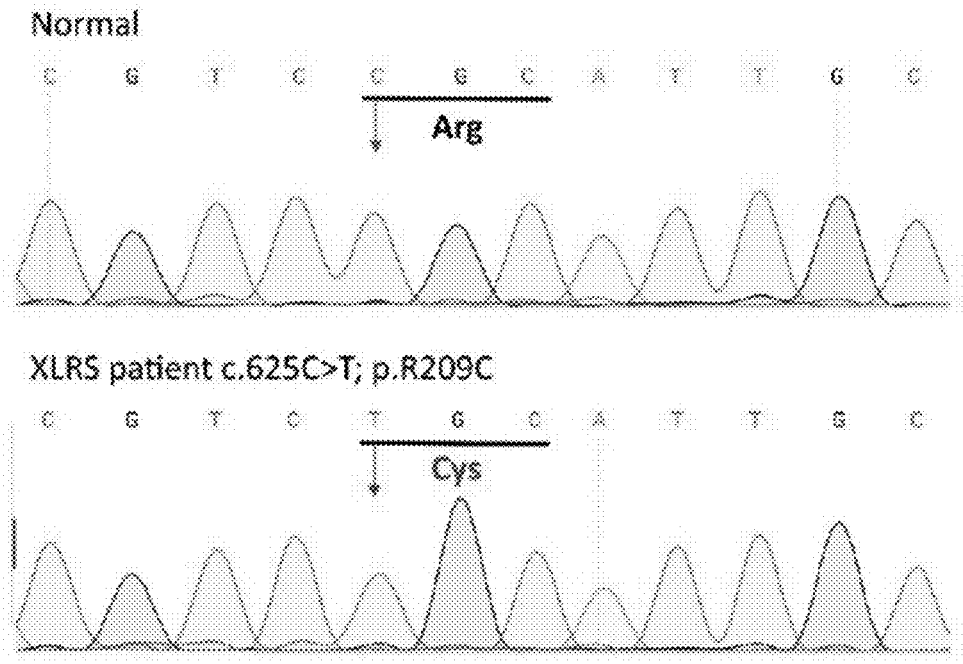

Fig. 1A

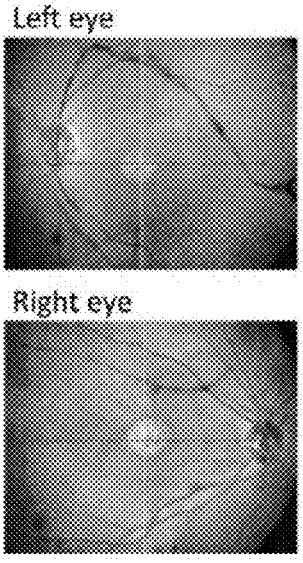

Fig. 1B

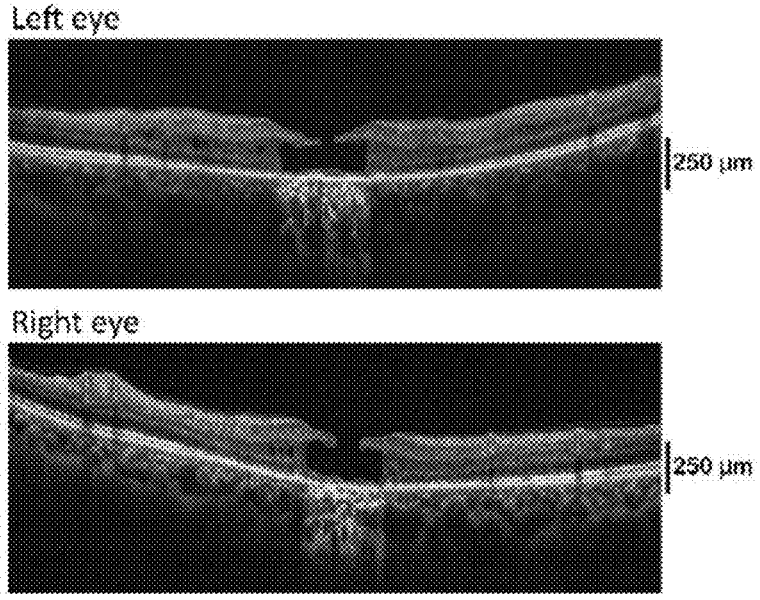

Fig. 1C

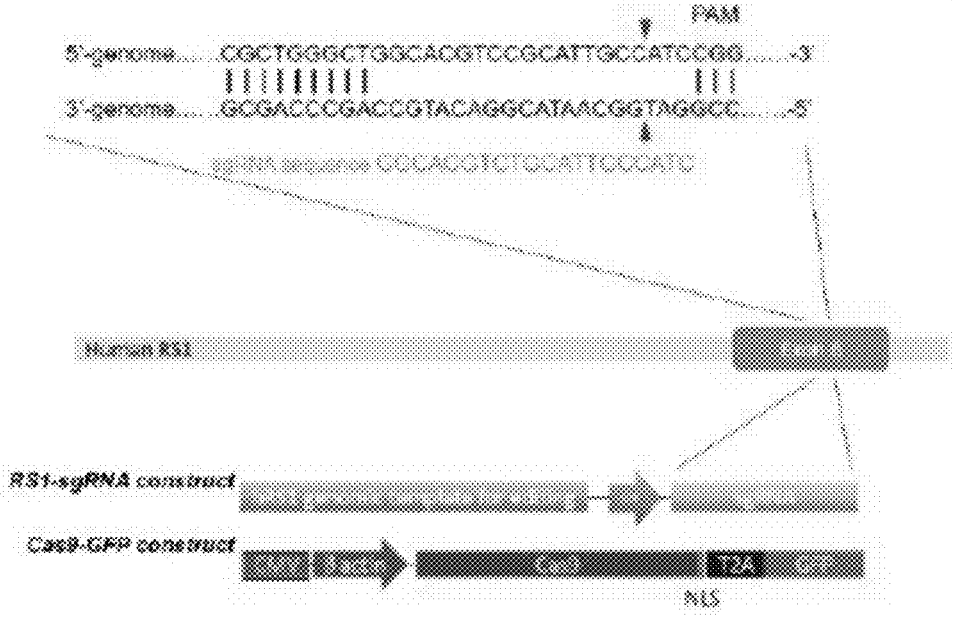
PAM
5'-genome....
3'-genome....
RS1-sgRNA construct
Cas9-GFP construct
NLS

Fig. 2A

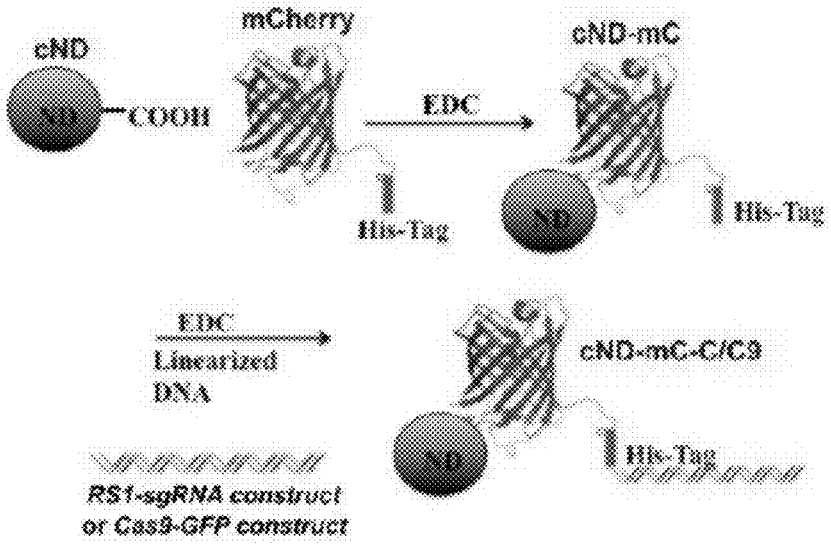
cND
COOH
mCherry
EDC
cND-mC
His-Tag
His-Tag
EDC
Linearized
DNA
cND-mC-C/C9
His-Tag
RS1-sgRNA construct
or Cas9-GFP construct

Fig. 2B

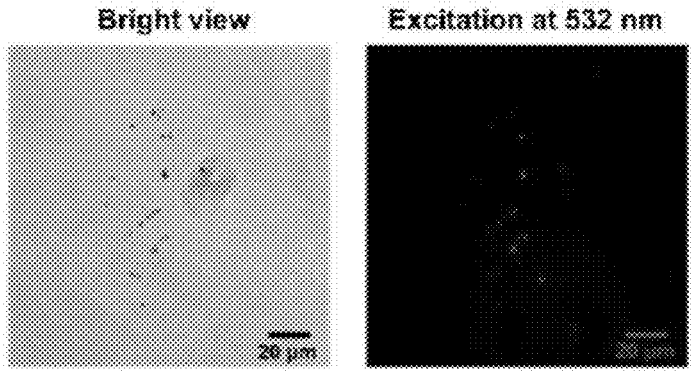
Bright view
Excitation at 532 nm
20 μm

Fig. 2C

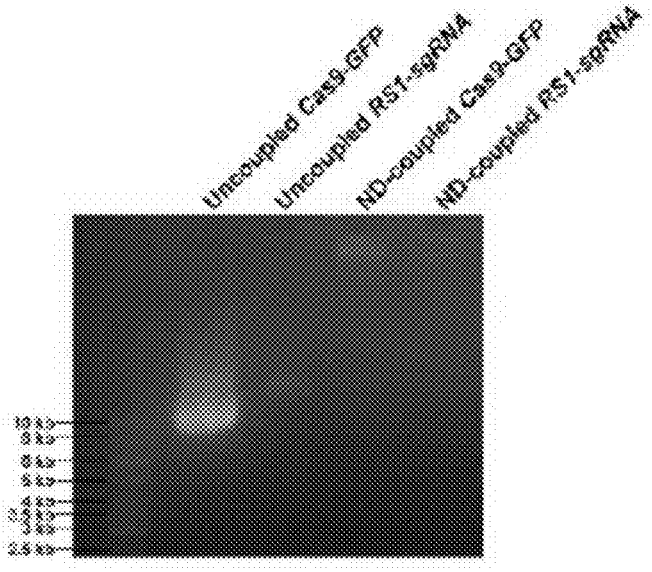
Uncoupled Cas9-GFP
Uncoupled RS1-sgRNA
ND-coupled Cas9-GFP
ND-coupled RS1-sgRNA

Fig. 2D

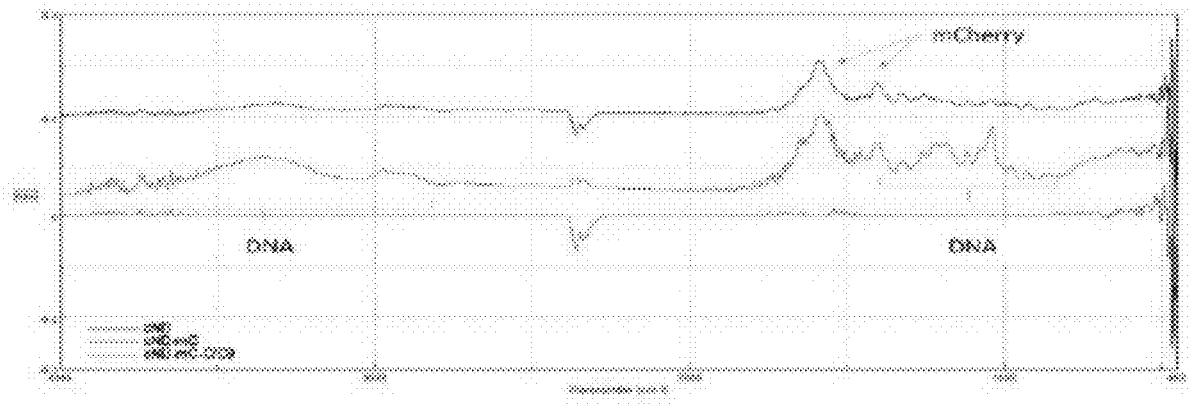

Fig. 2E

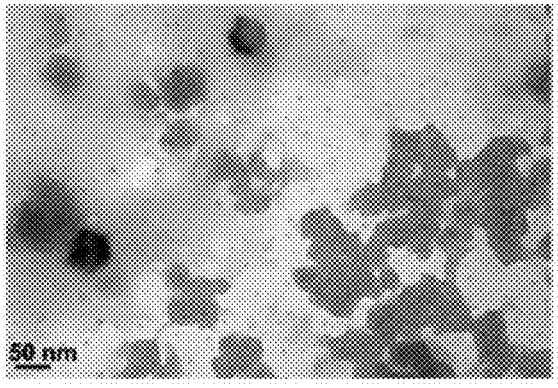

Fig. 2F

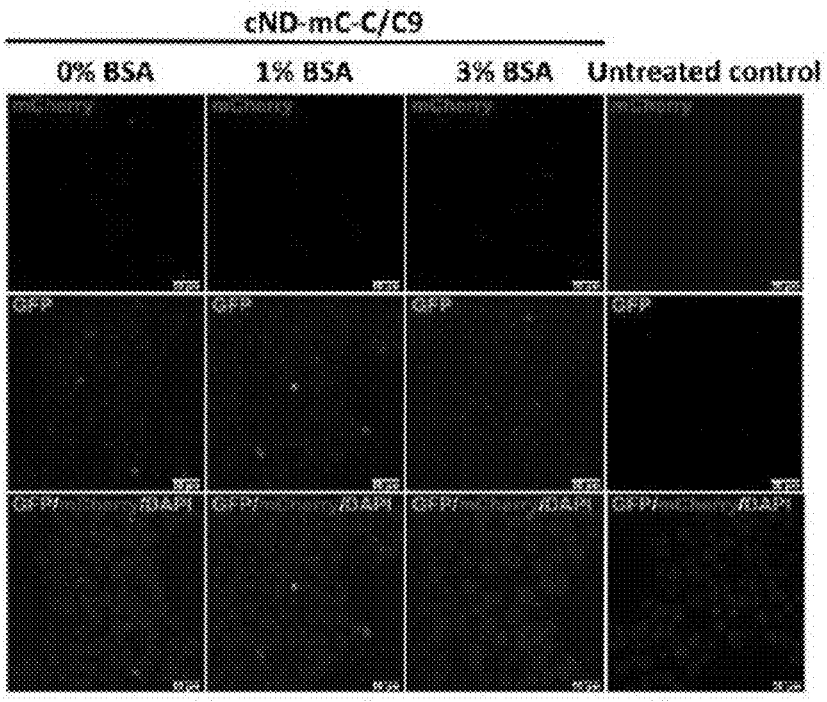

Fig. 3A

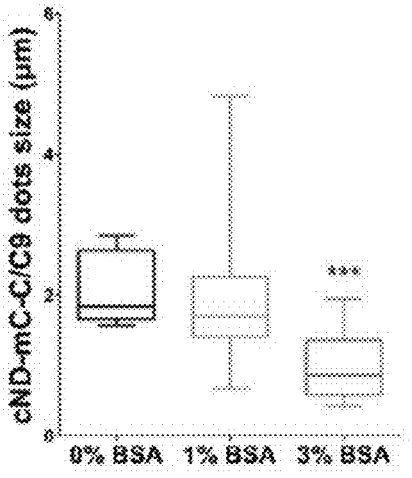

Fig. 3B

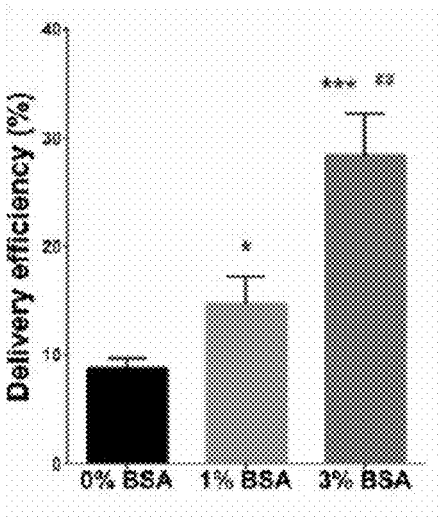

Fig. 3C

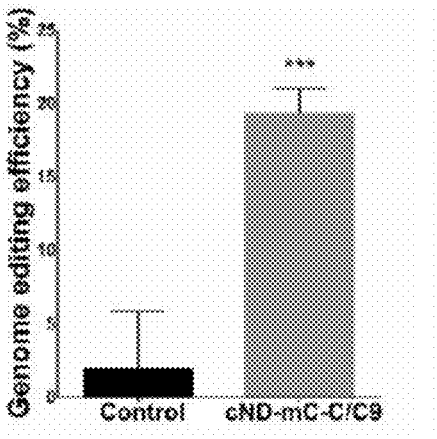
Genome editing efficiency (%)
***
Control
cND-mC-C/C9

Fig. 3D

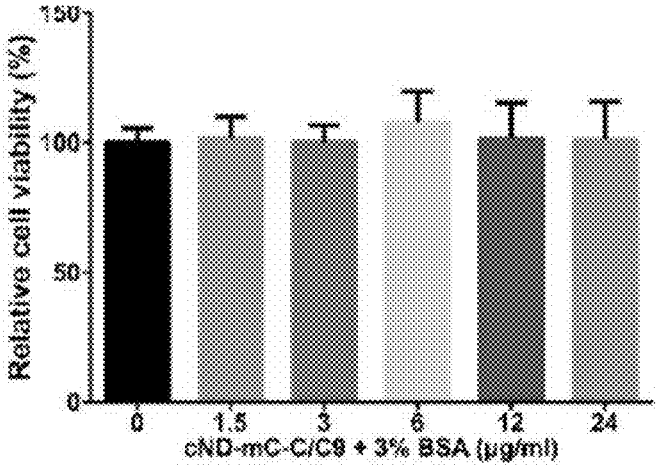
Relative cell viability (%)
150
100
50
0
0
1.5
3
6
12
24
cND-mC-C/C9 + 3% BSA (μg/ml)

Fig. 3E

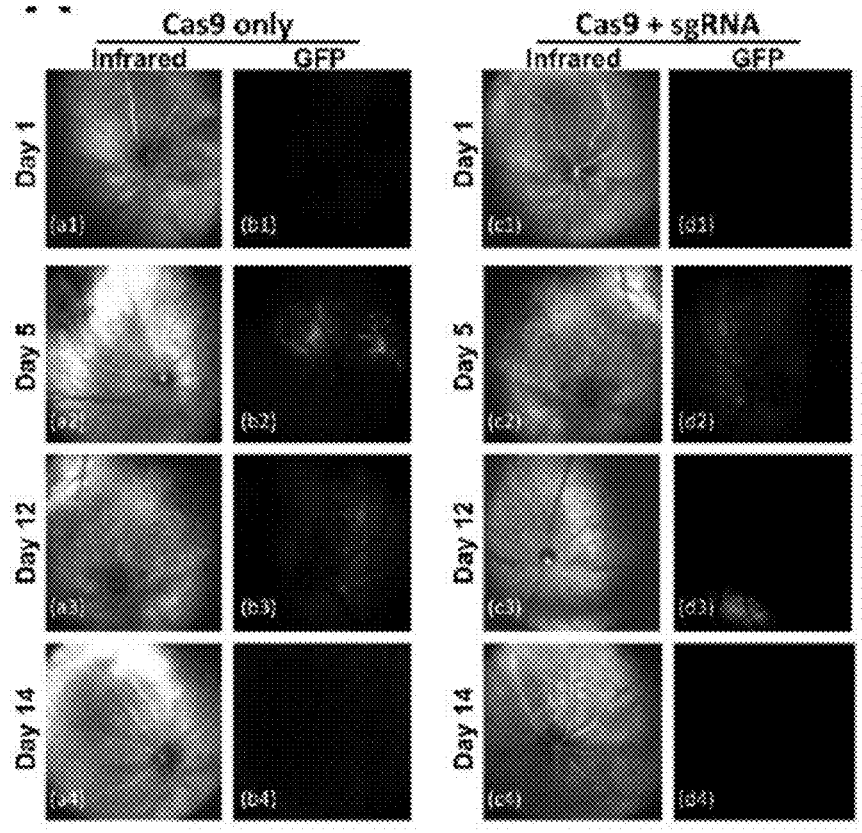
Cas9 only
Infrared
GFP
Cas9 + sgRNA
Infrared
GFP
Day 1
Day 5
Day 12
Day 14
(a1)
(b1)
(c1)
(d1)
(b2)
(d2)
(b3)
(d3)
(b4)
(d4)

Fig. 4A

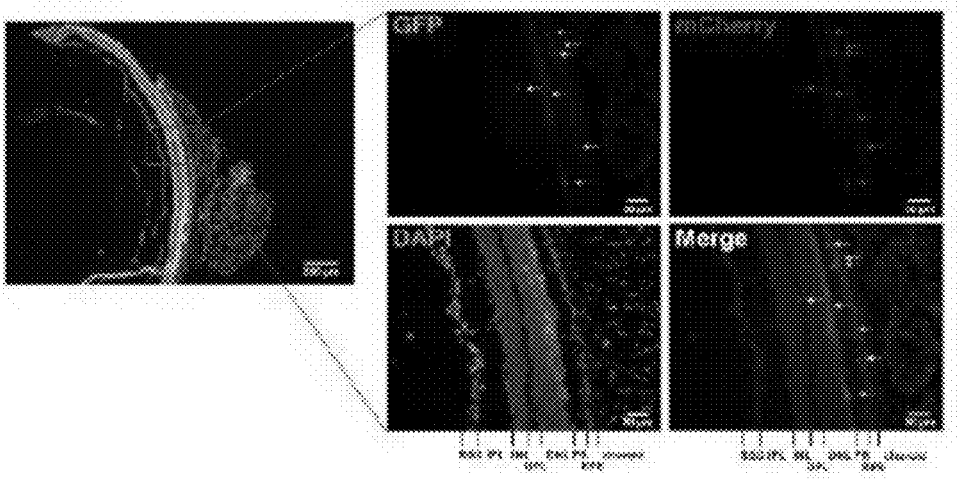
GFP
DAPI
Merge

Fig. 4B

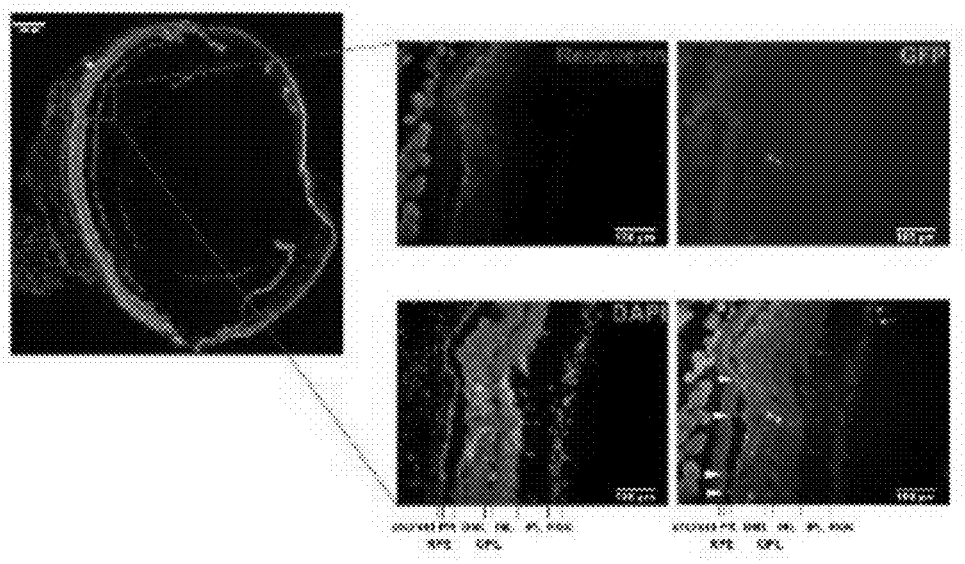

Fig. 4C

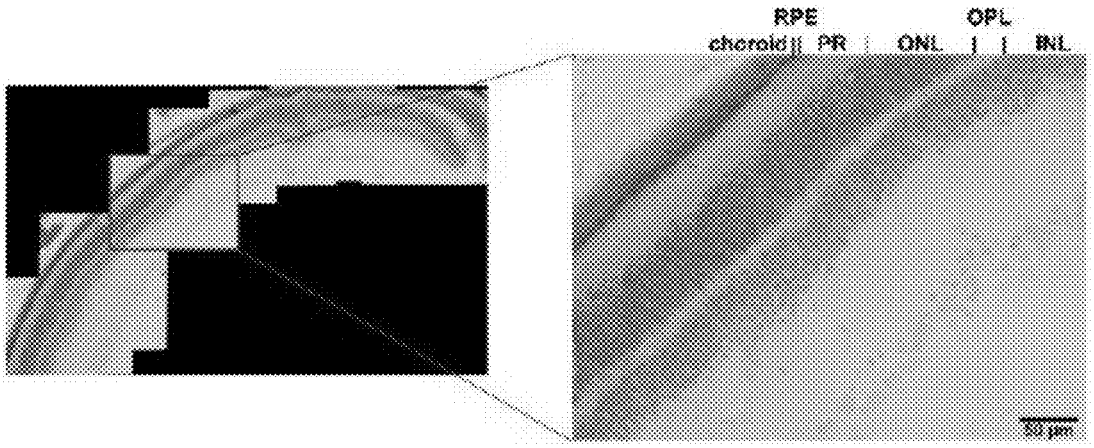

Fig. 4D

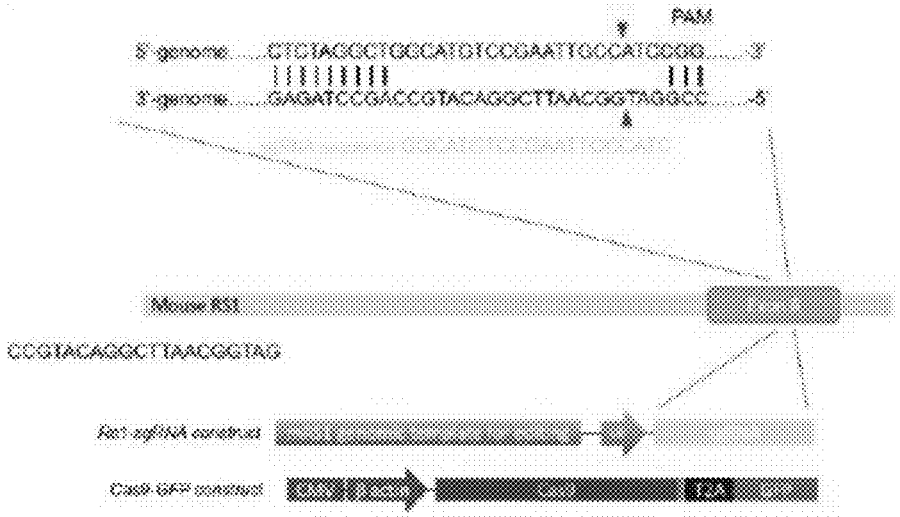

Fig. 5A

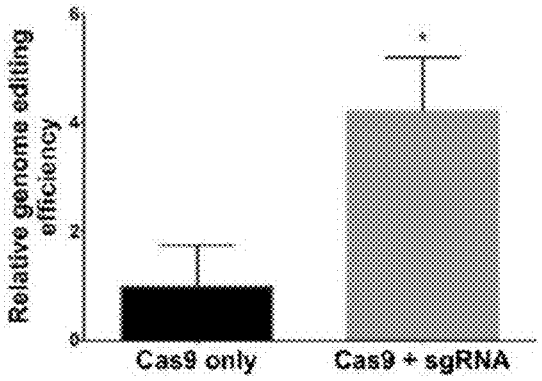

Fig. 5B

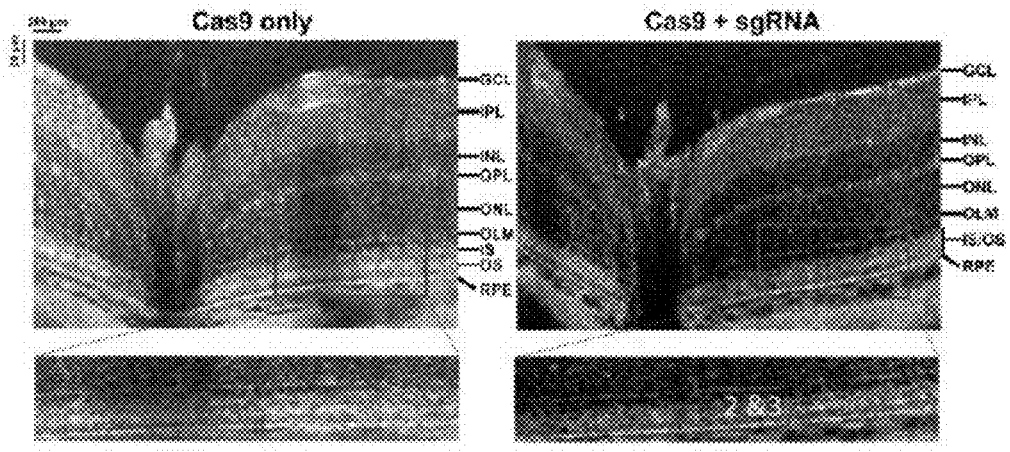

Fig. 5C

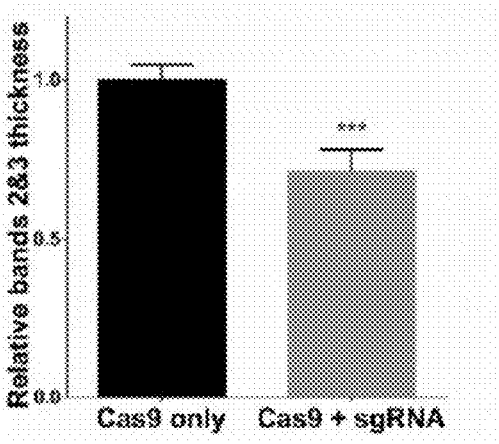

Fig. 5D

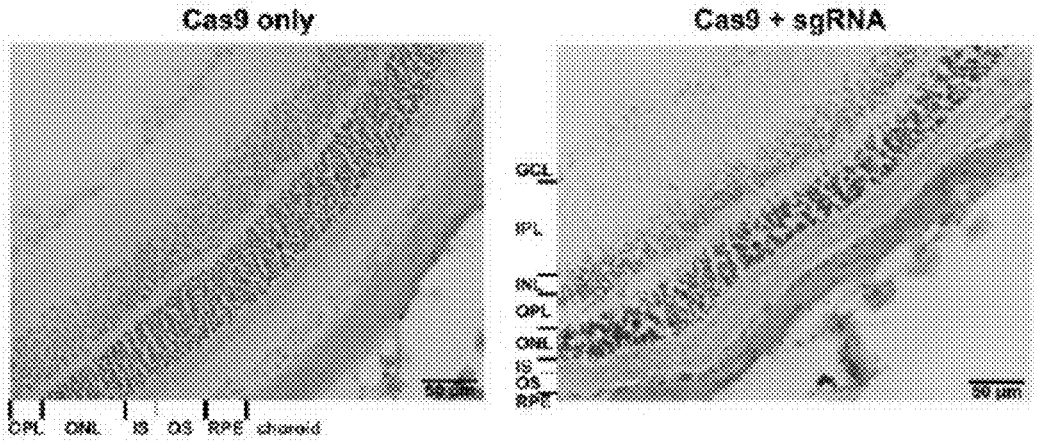

Fig. 5E

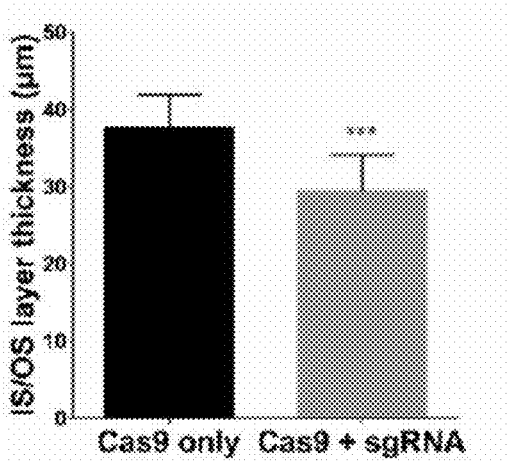

Fig. 5F

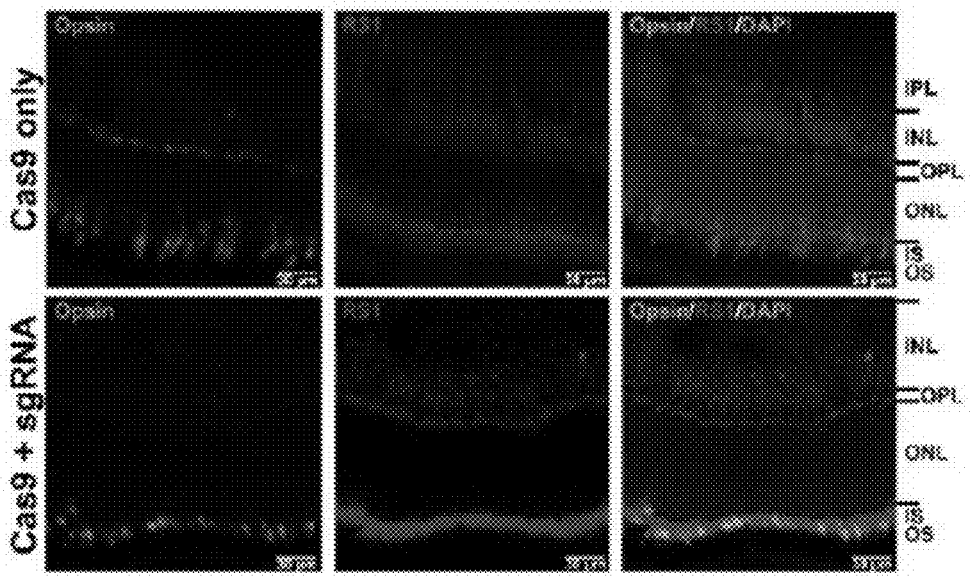
Cas9 only
Cas9 + sgRNA
IPL
INL
OPL
ONL
IS
OS

Fig. 6A

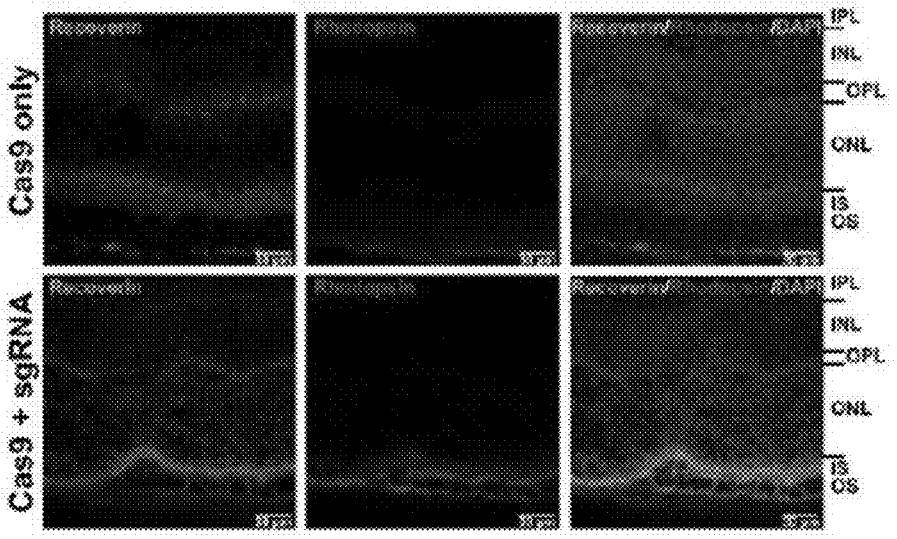
Cas9 only
Cas9 + sgRNA
IPL
INL
OPL
ONL
IS
OS

Fig. 6B

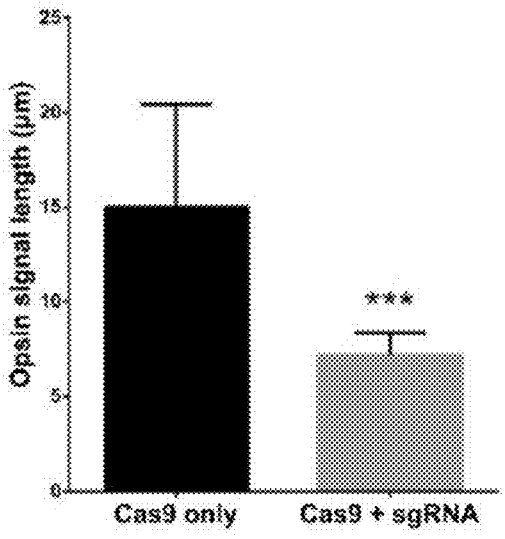

Fig. 6C

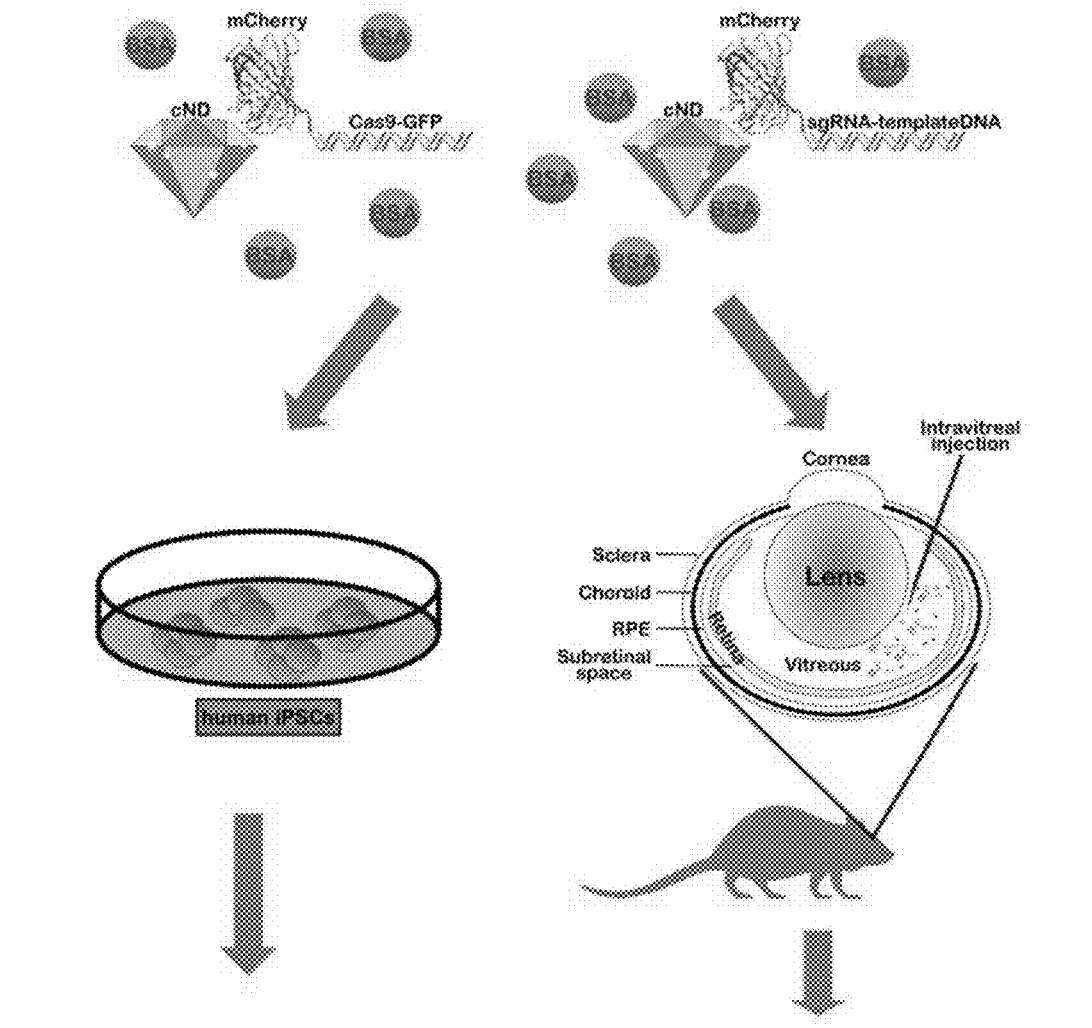
mCherry
cND
Cas9-GFP
mCherry
cND
sgRNA-templateDNA
Intravitreal injection
Cornea
Sclera
Choroid
RPE
Subretinal space
Retina
Lens
Vitreous
human iPSCs
• Internalization (mCherry)
• Gene expession (GFP)
• Specific RS1 gene editing (ddPCR)
• Internalization (mCherry)
• Gene expession (GFP)
• Specific Rs1 gene editing (ddPCR)
• Specific phenotype (OCT, H&E)

Fig. 7

CARBOXYLATED NANODIAMOND-MEDIATED CRISPR-CAS9 DELIVERY SYSTEM

REFERENCE TO SEQUENCE LISTING SUBMITTED VIA EFS-WEB

[0001] This application includes an electronically submitted sequence listing in .txt format. The .txt file contains a sequence listing entitled "2020-12-16_5992-0297PUS2_ST25" created on December 16, 2020 and is 3,240 bytes in size. The sequence listing contained in this .txt file is part of the specification and is hereby incorporated by reference herein in its entirety.

FIELD OF THE INVENTION

[0002] The present invention pertains to a CRISPR-Cas9 delivery System for delivering some components for treating a disease or repairing a tissue damage.

BACKGROUND OF THE INVENTION

[0003] X-linked juvenile retinoschisis (XLRS) is a common hereditary macular degeneration that affects the vision of young boys, with a prevalence of 1 in 5,000 to 1 in 25,000 [1, 2]. The clinical features of XLRS include early vision loss associated with bilateral foveae and splitting of the inner retinal layer, retinal detachment, and vitreous hemorrhage [3]. RS1, the gene associated with XLRS, contains six exons and encodes a protein of 224 amino acids [4]. More than one hundred RS1 mutations have been confirmed to be associated with the development of XLRS, and this result also indicates a high degree of clinical variability (http://www.dmd.nl/rs).

[0004] The protein structure of RS1 is composed of N-terminal secretory leader sequence and discoidin domain in C-terminal region, which are highly conserved across species [5, 6]. The discoidin domain is found in a number of secreted or membrane-bound proteins and is known to be involved in cell adhesion and cell-cell interaction [7]. Most of the mutations in the RS1 gene are missense mutations, although nonsense mutations, deletions, insertions, and splice site mutations are also found [8, 9]. Previous studies have indicated that the patients with RS1 missense mutations Asp145His, Arg102Gln, Arg209His and Arg213Gln exhibit severe retinoschisis characteristics in the clinic [10, 11]. Missense mutations in the RS1 protein cause misfolding and may cause intracellular and extracellular protein accumulation, ultimately leading to cystic and schisis structures in the retina [12]. RS1 is expressed and secreted by photoreceptors of the outer retina and bipolar cells of the inner retina, as was observed in the retina of mice [13]. Further studies have shown that RS1 attaches to the surface of retinal cells after synthesis and secretion by photoreceptors and mediates adhesion between photoreceptor cells, bipolar cells and Muller cells, thereby promoting the maintenance of structural integrity of the retina [14].

[0005] Nanodiamond (ND) is a carbon-based nanomaterial that can be used to carry biomolecules and chemicals [15-17]. In order to achieve the goal of multi-functional delivery by NDs, several techniques have been developed to promote conjugation of chemicals to the surface by introducing carboxyl, hydroxyl and thiol groups. Many studies have reported that NDs can also be used as a delivery system for biomolecules, such as DNA [18, 19], proteins [20, 21], and small molecule drugs [22, 23]. ND's biocompatibility and non-toxicity makes it a relatively safe nanomaterial for biomedical applications [24]. These advantages of NDs make it a promising carrier of therapeutic agents to treat hereditary retinal diseases.

[0006] The application of NDs for the treatment of human diseases is promising, but the U.S. Food and Drug Administration (FDA) still requires that the agents injected into the body do not accumulate for long periods of time [25]. Although fluorescently labeled NDs have an advantage of a stable fluorescent signal, a larger particle diameter is required to maintain the fluorescent sensitivity [26]. Animal experiments uncovered that larger sized particles may accumulate in organs, even without significant toxicity [27, 28]. The turnover of nanoparticles is an important issue in clinical applications. The production of urine by a kidney is an important way to eliminate them [29]. The threshold for the inorganic nanoparticles to filter molecules through the glomerular capillary wall is about 5.5 nm. Therefore, the size of the NDs may affect the efficiency of renal clearance [30].

[0007] It is desirable to develop a delivery system using a safe, efficient and traceable nanocarriers.

BRIEF DESCRIPTION OF THE DRAWINGS

[0008] The patent or application file contains at least one color drawing. Copies of this patent or patent application publication with color drawing will be provided by the USPTO upon request and payment of the necessary fee. The foregoing summary, as well as the following detailed description of the invention, will be better understood when read in conjunction with the appended drawings. For the purpose of illustrating the invention, there are shown in the drawings embodiments which are presently preferred.

[0009] In the drawings:

[0010] FIG. **1**A, FIG. **1**B and FIG. **1**C show the clinical characteristics of RS1 c.625C>T mutation carrier patient with X-linked juvenile retinoschisis (XLRS). FIG. **1**A (SEQ ID NOS: 5 and 6) shows the sanger sequencing results of the mutated RS1 locus in normal individual (top) and XLRS patient (bottom). The c.625C>T mutation in exon 6 of RS1 results in arginine to cysteine substitution. FIG. **1**B provides the ophthalmoscopy images of the eyes of XLRS patient showing a clear area of the chorioretinal atrophy involving the fovea. FIG. **1**C provides the OCT images revealing the presence of large cysts indicative the retinal degeneration

[0011] FIG. **2**A-FIG. **2**E shows the design of CRISPR-Cas9 constructs to introduce RS1 mutation and functionalization of mCherry-labeled NDs for their delivery. FIG. **2**A (SEQ ID NOS: 7, 8, and 9) provides the schematic showing the design of CRISPR-Cas9 constructs to introduce c.625C>T mutation into the human RS1 gene. The fragment of RS1 exon 6 sequence containing the cleavage site (red arrowhead) and PAM sequence (red font) shown at the top. The maps of two DNA constructs, Cas9-GFP and RS1-sgRNA, shown at the bottom. FIG. **2**B provides the scheme showing the design and production of CRISPR-Cas9-loaded NDs, wherein the carboxylated NDs (cNDs) were covalently linked to mCherry via COOH group in a reaction catalyzed by EDC to produce cND-mC, Cas9-GFP and RS1-sgRNA linear DNA was linked to cND-mC via His-tag to produce cND-mC-C/C9. FIG. **2**C provides a bright view and fluorescence microscopy image of cNDs coupled to mCherry. FIG. **2**D shows agarose gel showing migration of uncoupled

and ND-coupled Cas9-GFP and RS1-sgRNA DNA constructs. FIG. **2**E provides the FTIR spectra of the ND samples: cND (green line), cND-mC (blue line) and cND-mC-C/C9 (brown line). FIG. **2**F provides TEM image of BSA-mixed cND-mC-C/C9 nanoparticles.

[0012] FIG. **3**A-FIG. **3**E provide the editing of RS1 gene by cND-mC-C/C9 in hiPSCs. FIG. **3**A provides fluorescence microscopy images of hiPSCs treated with cND-mC-C/C9 nanoparticles mixed with the indicated concentrations of BSA. FIG. **3**B shows the measurement of the diameter of mCherry fluorescent dots inside hiPSCs on fluorescence microscopy images using ImageJ software. The means values are shown with standard deviation error bars. FIG. **3**C shows the quantification of delivery efficiency of cND-mC-C/C9 nanoparticles mixed with different concentrations of BSA. Expressed as the mean percentage of cells with internalized mCherry signal. FIG. **3**D provides ddPCR analysis of RS1 c.625C>T copy number in GFP-sorted population of cND-mC-C/C9-treated hiPSCs. FIG. **3**E provides the results of the CCK-8 cell viability assay showing the effect of treatment of hiPSCs with the indicated concentrations of cND-mC-C/C9affect their viability (Data expressed as relative to untreated (0 μg/ml). Statistical data shown as the means ±standard deviation error bars, *p<0.05, ***p<0.001, ##p<0.01 Student's t-test from 3 independent experiments. * versus 0% BSA, #3% BSA versus with 1% BSA).

[0013] FIG. **4**A-FIG. **4**D show the cND-mC-C/C9 delivery into the mouse retina. FIG. **4**A provides the SLO fundus image in mouse eyes injected with cND-mC-C/C9 nanoparticles carrying Cas9-GFP (Cas9 only) and RS1-sgRNA (Cas9+sgRNA) DNA constructs. FIG. **4**B provides Fluorescence microscopy observation of localization of mCherry and green fluorescent protein (GFP) signals in transverse section of cND-mC-C/C9-treated mouse retina. GFP and mCherry signals are indicated by arrows. FIG. **4**C provides Fluorescence microscopy observation of expression of GFP expression in transverse section of cND-mC-C/C9-treated mouse retina. GFP signals were observed in RGC layer (yellow arrows), photoreceptor/Müller cell layer (red arrows), and RPE layer (white arrowheads). Recoverin, the marker of photoreceptors, is immunostained in red. Nuclei stained with DAPI. FIG. **4**D provides H&E staining of the section of cND-mtwC-C/C9-treated mouse retina. RPE—retinal pigment epithelium, PR—photoreceptors, ONL—outer nuclear layer, OPL—outer plexiform layer, INL—inner nuclear layer, IPL—inner plexiform layer, RGC—retinal ganglion cells.

[0014] FIG. **5**A-FIG. **5**D show the editing of Rs1 gene by cND-mC-C/C9 in the mouse retina. FIG. **5**A (SEQ ID NOS: 10, 11, 12 and 13) provides the scheme showing the design of CRISPR-Cas9 constructs to introduce c.625C>T mutation into the mouse Rs1 gene. The fragment of Rs1 exon 6 sequence containing the cleavage site (red arrowhead) and PAM sequence (red font) shown at the top. The maps of two DNA constructs, Cas9-GFP and Rs1-sgRNA, shown at the bottom. FIG. **5**B shows the results of the ddPCR analysis of Rs1 c.625C>T copy number in retinas treated for two weeks with control (Cas9 only) and Rs1-targeting cND-mC-C/C9 nanoparticles (Cas9+sgRNA). Data are expressed as relative to control. FIG. **5**C provides OCT images of mouse retinas treated for two weeks with control (Cas9 only) and (Cas9+sgRNA) cND-mC-C/C9 nanoparticles. Retinal layers shown to the right: GCL—ganglion cell layer, IPL—inner plexiform layer, INL—inner nuclear layer, ONL—outer nuclear layer, OPL—outer plexiform layer, OLM outer limiting membrane, IS—inner segments, OS—outer segments, RPE—retinal pigment epithelium. Bottom image: zoom in of the area of the top image surrounded by red rectangle, showing the structure of hyperreflective outer retinal bands 2 and 3. FIG. **5**D provides the quantification of thickness of hyperreflective outer retinal bands 2 and 3 in OCT images in FIG. **4**C. The data expressed as means vale measurements, "Cas9+sgRNA" quantified relative to "Cas9 only" control. FIG. **5**E provides the H&E staining of cross sections of mouse retinas treated for two weeks with control (Cas9 only) and (Cas9+sgRNA) cND-mC-C/C9 nanoparticles. FIG. **5**F shows the quantification of thickness of IS/OS layer in OCT images in FIG. **5**E. The data expressed as means from 3 measurements, "Cas9+sgRNA" quantified relative to "Cas9 only" control.

[0015] FIG. **6**A-FIG. **6**C show the effect of cND-mC-C/C9-mediated Rs1 editing on photoreceptor cells in the mouse retina. Immunofluorescence staining of the cross sections of the mouse retinas treated with the control cND-mC-C/C9 particles (Cas9 only) and cND-mC-C/C9 particles targeting Rs1 gene (Cas9+sgRNA). The layers of the retina indicated on the right: IPL—inner plexiform layer, INL—inner nuclear layer, OPL—outer plexiform layer, ONL—outer nuclear layer, IS—inner segments, OS—outer segments. Nuclei labeled with DAPI. FIG. **6**A shows Immunostaining with antibodies against cone cell-specific opsins (Opsin) and RS1. FIG. **6**B shows the immunostaining with antibodies against recoverin and rhodopsin. FIG. **6**C shows the quantification of the length of immunofluorescent signals of cone cell-specific opsins.

[0016] FIG. **7** shows the summary of the study, wherein the nanodiamonds were functionalized to covalently attach mCherry protein and DNA constructs encoding components of CRISPR-Cas9 genome editing system. Nanoparticles were mixed with BSA and used to edit the genomes of iPSCs and mouse retinas, thus making them a useful tool to create the in vitro and in vivo disease models, respectively.

SUMMARY OF THE INVENTION

[0017] Accordingly, the present invention provides a highly efficient delivery system for gene editing.

[0018] In one aspect, the present invention provides a delivery system for gene editing comprising nanodiamond (ND) particles as the carriers of CRISPR-Cas9 components including a Cas9 protein, a guide protein (gRNA), a template DNA designed to introduce the mutation in a given gene for repairing a tissue damage, wherein the ND particles have a diameter less than 5 nm, and functionalized by carboxylation of the surface and covalently conjugated with a fluorescent protein; and a first linear DNA construct for expression of the Case 9 protein, and a second linear DNA construct for expression of the gRNA/template DNA were linked with the ND particles covalently conjugated with the fluorescent protein by phosphoryl imidazole to obtain carboxylated nanodiamond-mediated CRISPR-Cas9 ND particles.

[0019] In one example of the invention, the ND particles have a diameter in a range of 3 nm-5 nm; preferably the ND particles have a diameter of about 3 nm.

[0020] In one example, the fluorescent protein as used in the invention is a mCherry protein.

[0021] In one particular example, the carboxylated nanodiamond-mediated CRISPR-Cas9 ND particles according to the invention may be coated by bovine serum albumin (BSA) before using. It was unexpectedly found that the delivery efficiency of NDs is increased and the diameter of of mCherry fluorescent dots, indicative of less aggregated state, is decreased.

[0022] In one example, the given gene is RS1 gene associated with X-linked retinoschisis (XLRS).

[0023] According to the invention to create a disease model, the mutation in the given gene is introduced via two linear DNA constructs, which are attached to the conjugated mCherry, and the first linear DNA construct encodes for Cas9 endonuclease and a green fluorescent protein (GFP) reporter, and the second linear DNA construct encodes for a sgRNA and contains an insert of HDR template designed to introduce RS1 c.625C>T mutation.

[0024] In the invention, the the delivery leads to introduction of RS1 c.625C>T mutation in human iPSCs or mouse retinas.

[0025] In another aspect, the invention provides a method for treating a disease or repairing a tissue damage in a subject, comprising delivering and internalizing the mutation in a given gene into said subject through the system of the invention.

[0026] In one example, the disease is X-linked retinoschisis (XLRS), and the given gene is RSI gene associated with X-linked retinoschisis (XLRS).

[0027] In a further aspect, the invention provides a method for creating an in vitro or in vivo disease model, comprising delivering and internalizing the mutation in a given gene into induced pluripotent stem cells (iPSCs) or an animal organ through the system of the invention.

[0028] In one example, the disease is X-linked retinoschisis (XLRS), the given gene is RSI gene associated with X-linked retinoschisis (XLRS), and the animal organ is mouse retinas.

[0029] In one example of the invention, the delivery leads to an introduction of RS1 c.625C>T mutation into human iPSCs or mouse retinas.

[0030] According to the invention, the Rs1 gene editing in the mouse retinas results in several pathological features typical for XLRS, such as aberrant photoreceptor structure.

[0031] It is to be understood that both the foregoing general description and the following detailed description are exemplary and explanatory only and are not restrictive of the invention.

DETAILED DESCRIPTION OF THE INVENTION

[0032] Unless defined otherwise, all technical and scientific terms used herein have the same meaning as commonly understood by a person skilled in the art to which this invention belongs.

[0033] Nanodiamond (ND) particles can be used as a drug delivery vehicle characterized by high biocompatibility, loading capacity and cell penetration. The non-covalent methods of ND-oligonucleotide conjugation can be used to prepare the NDs, and the covalent bond of the nucleic acid through the peptide contributes to the stability, accessibility and selectivity of the conjugate. In the present invention, the ND-based CRISPR-Cas9 delivery vector was designed by functionalizing ND surface with a carboxyl (COOH) group, conjugating 6His-tagged mCherry reporter protein to the ND via the peptide bond, and covalently attaching linear DNA encoding green fluorescent protein (GFP) reporter and components of CRISPR-Cas9 system via the phosphoryl imidazole bond between 5'-phosphate of DNA and imidazole group of histidine of 6His-tag. Since internalization of nanoparticles usually undergoes via the endosome pathway, mCherry was chosen to construct the backbone of the delivery vector to monitor the transfection efficiency, because it constitutively exhibits red fluorescence even in the acidic environment (pH 5-6) of the late endosomes, unlike GFP, whose green fluorescence is quenched at such pH values. At the same time, GFP was designed to be expressed from a conjugated DNA, as a reporter of successful delivery and functional effects of cargo DNA.

[0034] As used herein, the term "nanodiamonds (NDs)," "nanodiamond (ND) particles" or "diamond nanoparticles" refers to particles having a shape of diamond with a size below 1 micrometre, which can be produced by impact events such as an explosion or meteoritic impacts, and are potential for surface functionalization. As being inexpensive, large-scale synthesis, they are potential for surface functionalization. the ND particles can be used as a drug/biomaterial delivery vehicle characterized by high biocompatibility, loading capacity and cell penetration. The non-covalent methods of ND-oligonucleotide conjugation can be used to prepare the NDs, and the covalent bond of the nucleic acid through the peptide contributes to the stability, accessibility and selectivity of the conjugate.

[0035] In one example of the present invention, the ND-based CRISPR-Cas9 delivery vector was designed by functionalizing ND surface with a carboxyl (COOH) group, conjugating 6His-tagged mCherry reporter protein to the ND via the peptide bond, and covalently attaching linear DNA encoding GFP reporter and components of CRISPR-Cas9 system via the phosphoryl imidazole bond between 5'-phosphate of DNA and imidazole group of histidine of 6His-tag. Since internalization of ND particles usually undergoes via the endosome pathway, mCherry was chosen to construct the backbone of the delivery vector to monitor the transfection efficiency, because it constitutively exhibits red fluorescence even in the acidic environment (pH5-6) of the late endosomes, unlikeGFP, whose green fluorescence is quenched at such pH values. At the same time, GFP was designed to be expressed from a conjugated DNA, as a reporter of successful delivery and functional effects of cargo DNA. We demonstrated that the mCherry protein carried by cNDs was stable in the mouse retina for up to two weeks. In addition, the GFP reporter gene was also continuously expressed in vivo from plasmid DNA. In order to ensure more efficient transfection by nanocarriers, they often need to be stabilized with additional materials.

[0036] It was found in the present invention that bovine serum albumin (BSA) increased delivery efficiency of cNDs in a concentration dependent manner, as well as decreased the diameter of mCherry fluorescent dots, indicative of less aggregated state (see FIG. **3**).

[0037] CRISPR-Cas9-mediated genome editing of the pluripotent stem cells, including embryonic stem cells (ESCs) and induced pluripotent stem cells (iPSCs), offers a great potential for modelling human genetic diseases as they can be differentiated into any tissue affected by the pathology. In the present invention, the cND-based approach can be utilized to safely and efficiently deliver CRISPR-Cas9 components to human iPSCs. By using our cND-mC-C/C9

delivery system, we could successfully introduce XLRS-specific mutation of RS1 gene (c.625C>T) into normal human iPSCs. In the future, such knock-in iPSCs can be used to study the molecular and cellular mechanisms of retinopathy by differentiating them into 3D retinal organoids and using parental iPSCs as a control with the same genetic background.

[0038] XLRS is the X-linked retinopathy caused by mutations in RS1 gene and characterized by splitting of the retinal layers. In previously characterized Rs1-knockout mouse model, several pathological features were demonstrated, including outer nuclear layer (ONL) thickness reduction and inner retinal cavitation. In the present invention, OCT imaging of mouse retinas treated with cND-mC-C/C9 nanoparticles did not reveal the presence of cysts in the retina, however, we clearly observed the merger of hyperreflective outer retinal bands 2 and 3, indicative of aberrant photoreceptor structure. Consistently, the analysis of retinal tissue sections revealed reduction of thickness of outer retinal layer and shortened morphology of photoreceptor cells. A partial human mutant Rs1 gene in adult male mice were prepared to show a phenotype of changes in the outer segment of the photoreceptor cells, which supports the idea that Rs1 gene inactivation may directly cause photoreceptor damage. Whereas intravitreal injection leads to exposure of all retinal cell types to the NDs, only the morphology of the photoreceptor layer was affected by it, thus corroborating the functional specificity of RS1 protein as the crucial factor for organization of the outer retina. On the other hand, the specificity of our ND-based vector to target the specific cell type, like photoreceptors, can potentially be increased by using the advantages of the design of this vector. As we used the COOH groups of the carboxylated NDs to covalently attach the mCherry reporter marker via the peptide bond, the cell-type specific ligand proteins can be concomitantly conjugated to target the NDs to the photoreceptor-specific surface markers.

[0039] Whereas the disadvantage of the ND-based vectors in comparison with the virus-based systems is their low transfection efficiency, their advantage is based on the higher safety as an inert and low immunogenicity material. By using scanning laser ophthalmoscopy, we observed that GFP signal persisted in the mouse retina for up to 12 days after the intravitreal injection of the NDs (FIG. **3**A). Therefore, given higher safety of the NDs, we can speculate that the efficiency of in vivo genome editing can be increased by constantly maintaining high concentration of the NDs by injecting them once GFP signal is diminished.

[0040] The present invention is further illustrated by the following examples, which are provided for the purpose of demonstration rather than limitation.

EXAMPLE

[0041] 1.1. CRISPR-Cas9 Design

[0042] The Cas9-GFP expression vector was described in a previous study [31]. The human RS1 c.625 C>T (p.R209C) mutation was introduced using the following sgRNA scaffold sequence:

(SEQ ID NO: 1)

GGCACGTCTGCATTGCCATCGTTTTAGAGCTAGAAATAGCAAGTTAAAAT

AAGGCTAGTCCGTTATCAACTTGAAAAAGTGGCACCGAGTCGGTGC;

and the following HDR sequence:

(SEQ ID NO: 2)

GTCTTCTATGGCAACTCGGACCGCACCTCCACGGTTCAGAACCTGCTGCG

GCCCCCCATCATCTCCCGCTTCATCCGCCTCATCCCGCTGGGCTGGCATG

TCCGGATTGCCATCCGGATGGAGCTGCTGGAGTGCGTCAGCAAGTGTGCC

TGATGCCTGCCTCAGCTCGGCGCCTGCCAGGGGGTGACTG.

[0043] The mouse Rs1 c.625 C>T was introduced using sgRNA scaffold sequence:

(SEQ ID NO: 3)

GGCATGTCCGAATTGCCATCGTTTTAGAGCTAGAAATAGCAAGTTAAAAT

AAGGCTAGTCCGTTATCAACTTGAAAAAGTGGCACCGAGTCGGTGC;

and HDR sequence:

(SEQ ID NO: 4)

GTCTTCTATGGAAACTCAGACCGGAGTTCTACAGTTCAGAACTTACTCAG

GCCCCCCATCATTTCCCGCTTCATCCGACTGATCCCTCTAGGCTGGCACG

TCtGtATTGCCATCCGGATGGAGCTGCTTGAGTGTGCCAGCAAGTGTGCC

TGATGTCTATTTCAGCTCAGTTCTGTCACTTGCAGGGAGA.

[0044] The sgRNA scaffold and HDR sequences were cloned into pUC57 vector (Addgene).

[0045] 1.2. Preparation of Carboxylated Nanodiamond (cND) and Linkage with mCherry and Linear DNA

[0046] The detonation nanodiamonds (NDs) were purchased from NanoCarbon Institute Co., Ltd in the form of 2.5% (w/v) water colloidal solution. According to the specifications of the supplied colloidal solution, it contains particles of the size distribution around 3.2 ±0.6 nm. Formation of graphene on ND surface and the minute contamination from zirconia beads and metal ions from the detonation chamber are present, but of little or no harm to this research. In order to functionalize the surface of NDs with carboxyl (COOH) group, they were treated with 3:1 mixture of H2SO4 and HNO3 with stirring at 100° C. for 72 h. The resultant carboxylated NDs (cNDs) were washed several timed in double-distilled water and suspended in PBS at a concentration of 250 μg/ml. mCherry protein was linked to cNDs by peptide with 1-ethyl-3-(3-dimethylaminopropyl) carbodiimide (EDC) used as a catalytic agent. cNDs (250 μg/m1 suspension in PBS), mCherry protein (250 μg/m1), and 0.1 M ECD were mixed at a volume ratio of 1:2:3 and incubated on a rolling shaker at 4° C. for 18 h. The reaction products (cND-mCherry) were purified by dialysis against PBS for another 18 h. mCherry and linear DNA were linked by phosphoryl imidazole bond between imidazole group from mCherry 6His-tag tail and DNA phosphate group. cND-mCherry PBS solution (about 40 μg/m1), linearized DNA constructs (200 μg/m1) and 0.1 M ECD were mixed at a volume ratio of 5:2:1 and incubated on a rolling shaker at 4° C. for 18 h. The reaction products were purified by dialysis against PBS for another 18 h. Prior to applying the loaded NDs to the cells, bovine serum albumine (BSA) was added to a final concentration of 1 or 3% (w/v), and nanoparticles were sonicated for 2 h to prevent their aggregation and ensure even dispensing.

[0047] 1.3. Transmission Electron Microscopy (TEM) and Fourier Transform Infrared Spectroscopy (FTIR)

[0048] TEM images of the NDs were obtained on a JEM-2000EX II (JEOL) run at 100 kV. NDs (40 μg/mL) were suspended in PBS and then pipetted onto a copper TEM grid (Ted Pella Inc.) and the solvent was removed after overnight deposition. Surface modification of ND was detected by FTIR using FT/IR-4200 spectrometer (JASCO) with a scan size (resolution) of 4 cm-1 and 256 scans per sample.

[0049] 1.4. Human iPSCs

[0050] Human iPSCs were generated by reprogramming from peripheral blood mononuclear cells (PBMCs) of a healthy male Han Chinese donor as previously described [32]. Briefly, PBMCs were seeded into 24-well plates (5×10^5 cells/well) in complete PBMC medium. PBMCs were transduced with a mix of SeV vectors encoding OCT3/4, SOX2, KLF4 and cMYC at a multiplicity of infection (MOI) of 3. The medium was changed every second day, and on day 7 post transduction, 1.25×10^5 cells were plated onto a 10-cm dish precoated with a mouse embryonic fibroblast (MEF) feeder layer. On the next day, the medium was changed to hES medium and the cells were fed every other day for 7 days before switching to the daily feeding. Once the colonies emerged, they were mechanically dislodged and transferred to a fresh feeder. hiPSCs were cultured on Geltrex-coated cell culture dishes and incubated with mTeSR1 medium (STEMCELL Technologies). The cells were cultured in a 37° C. incubator containing 10% CO_2. The cells were cultured in a 37° C. incubator containing 10% CO 2. The hiPSCs cell line was characterized by typical iPSC morphology and positive alkaline phosphatase activity, expression of typical pluripotency markers as confirmed by RT-PCR and western blotting.

[0051] 1.5. Cell viability assay

[0052] The iPSCs were seeded in 96-well plates at 5×10^4 cells per well. After 24 h incubation, different doses of cND-mC-C/C9 mixed with BSA were added and incubated for 2 days. 10 μl of Cell Counting Assay Kit-8 solution (CCK-8, Sigma) was added to each well and incubated for 2 h. The absorbance at 490 nm was measured on a microplate reader. Cells treated with 10 μl of StemFlex medium (Thermo Fisher Scientific) instead of CCK-8 solution were used as a negative control. All experiments were performed independently three times.

[0053] 1.6. Animals

[0054] C57BL/6 male mice (6~10 weeks old) were purchased from National Laboratory Animal Center (Taipei, Taiwan). The mice were housed in a pathogen-free space and operated according to the National Research Council's Guide for the Care and Use of Laboratory Animals. All anesthesia and sacrifice procedures were reviewed and approved by the Animal Care and Use Committee of the Taipei Veterans General Hospital (TVGH). The mice were anesthetized with 250 mg/kg tribromoethanol (Sigma-Aldrich) by intraperitoneal injection, and placed under a dissecting microscope (SZX16, OLYMPUS, Japan) or spectral-domain OCT imaging system.

[0055] 1.7. Intravitreal Injection

[0056] Each mouse was intravitreally injected with 5 μl of different ND formulations into both eyes. The mix of NDs loaded with Cas9-GFP (15 ng/μl) and Rs1-sgRNA (30 ng/μl) constructs was administered unilaterally, and NDs loaded with Cas9-GFP (15 ng/ul) were administered to the contralateral eye as a control. A Hamilton syringe was used to inject 5 μl of the NDs into the vitreous cavity of an eye through the sclera behind the limbus of mice. During the procedure, about 5 μl of vitreous liquid was allowed to efflux through the puncture hole to allow the complete delivery of 5 μl of ND formulation.

[0057] 1.8. Spectral Domain OCT Imaging

[0058] The OCT images of the mouse retinas were obtained using a continuous, high-speed and high-resolution retinal image acquisition system (axial resolution, 7 μm; acquisition speed, 76 frames/s, 1000×1024 pixels in the X-Z plane) as previously described [33]. A horizontal scan of 400 images was obtained through the fundus.

[0059] 1.9. Droplet Digital PCR (ddPCR)

[0060] The genomic DNA copy number was quantified by ddPCR (BioRad). All primers and probe sequences (Suppl. Table 1) were designed on the OligoAnalyzer software (IDT). The ddPCR Supermix (no dUTP) for the probe was used in the droplets.

[0061] 1.10. Statistical Analysis

[0062] Unpaired Student's t-test was applied to assess numerical data statistical significance. Statistical significance was set at p-value less than 0.05. The calculations were performed using Excel software.

[0063] 2. Results

[0064] 2.1 The Design of CRISPR-Cas9 Constructs to Introduce RS1 Mutation and Functionalization of mCherry-Labeled NDs for their Delivery

[0065] In this study, we aimed to develop the approach of using NDs to create the disease model of XLRS by adapting them as a vehicle for the delivery of CRISPR-Cas9 genome editing system in order to modify XLRS-associated RS1 gene. The RS1 mutation c.625>T, leading to amino acid substitution p.R209C, is one of the known causative mutations in XLRS. The patient carrying this mutation (FIG. **1**A) was characterized by typical features of XLRS, such as clearly developed bilateral macular atrophy in the retina observed by ophthalmoscopy (FIG. **1**B), and typical schisis phenotype observed by optical coherence tomography (OCT) in both eyes (FIG. **1**C). To express the components of CRISPR-Cas9 editing system, two linear DNA constructs were designed. RS1-sgRNA construct contained a homology directed repair (HDR) template and encoded sgRNA directing the c.625>T mutation in exon 6 of RS1 gene (FIG. **2**A). Cas9-GFP construct encoded Cas9 endonuclease and GFP reporter (FIG. **2**A).

[0066] The original NDs were obtained by detonation method and their diameter was 3 nm. In order to attach the cargo, the surface of the NDs was functionalized by introducing the carboxyl groups using a strong oxidizing acid. The carboxylated NDs (cND) were then covalently linked with mCherry protein via the carboxyl groups, thus allowing fluorescent detection of these particles (cND-mC) (FIG. **2**B and FIG. **2**C). mCherry protein was designed to carry a polyhistidine tail to be used for covalent attachment of the 5'-phosphate group of linear DNA, encoding components of CRISPR-Cas9 editing system (FIG. **2**B). By agarose gel electrophoresis analysis, we showed that DNA was bound to the cND-mC particles (FIG. **2**D). By comparing the Fourier-transform infrared (FTIR) spectra of cND, cND-mC, and cND-mC-C/C9 nanoparticles, we found that the distinctive FTIR peak at 1640 cm^{-1} was observed in the latter two types, indicating the presence of mCherry protein (FIG. **2**E). At the same time, the peaks indicating the presence of DNA

moiety were observed in the FTIR spectrum of cND-mC-C/C9 nanoparticles (FIG. **2**D). The resultant NDs carrying mCherry and CRISPR-Cas9-encoding linear DNA (cND-mC-C/C9) were mixed with bovine serum albumin (BSA) to facilitate their delivery to cells and were observed by transmission electron microscopy (TEM), their average size, as determined by ImageJ, was 5.6+/−0.99 nm (FIG. **2**F).

[0067] 2.2 Editing of RS1 Gene by cND-mC-C/C9 in hiPSCs

[0068] As our initial objective, we aimed to use cND-mC-C/C9 nanoparticles to introduce the XLRS-associated RS1 mutation in human induced pluripotent stem cells (hiPSCs). Previous studies have shown that BSA stabilizes fluorescence brightness and prevents NDs from aggregation in phosphate buffer [34, 35]. Therefore, we treated hiPSC culture with cND-mC-C/C9 particles diluted in PBS with different concentrations of BSA (0%, 1% and 3%). To evaluate whether cND-mC-C/C9 nanoparticles were internalized by hiPSCs, the expression of fluorescent markers was observed under a fluorescent microscope. The fluorescence signals from both mCherry and GFP were observed inside the cells signifying that cND-mC-C/C9 particles were both internalized and the attached DNA was transcribed (FIG. **3**A). The average size of mCherry fluorescent dots was significantly smaller inside the cells treated with 3% BSA cND-mC-C/C9, indicating that mixing with BSA prevented particle aggregation (FIG. **3**B). Moreover, cND-mC-C/C9 mixed with 3% BSA were more efficiently delivered to the cells as compared to nanoparticles without BSA and mixed with 1% BSA (FIG. **3**C). Two days after the treatment of hiPSCs with cND-mC-C/C9 mixed with 3% BSA, GFP-expressing cells were sorted by flow cytometry. The RS1 c.625>T gene mutation in genomic DNA was analyzed by droplet digital PCR (ddPCR), and it was shown that this nucleotide was edited in ~19.3% of all alleles (FIG. **3**D). To test whether cND-mC-C/C9 have any toxic effects, hiPSCs were treated with different concentrations of 3% BSA-mixed cND-mC-C/C9 nanoparticles for two days, and their viability was assessed by CCK-8 assay. It was shown that in a range of concentrations between 1.5 and 24 μg/ml, cND-mC-C/C9 did not affect the viability of hiPSCs (FIG. **3**E). To summarize, these results indicate that the BSA-mixed cND-mC-C/C9 nanoparticles can be delivered to the hiPSCs, successfully edit their genome, and don't affect their viability.

[0069] 2.3 cND-mC-C/C9 Delivery into the Mouse Retina

[0070] To study the effects of cND-mC-C/C9 in vivo, we examined the distribution of nanoparticles in the mouse retina after cND-mC-C/C9 infusion. cND-mC-C/C9 particles mixed with 3% BSA were injected into the mouse eye by intravitreal injection and examined by scanning laser ophthalmoscopy (SLO) in live animals in a time course of two weeks. The fluorescence signals of GFP was clearly observed in the fundus of the retina, indicating to cND-mC-C/C9 internalization and expression (FIG. **4**A). Confocal microscopy of transverse retinal sections showed the presence of mCherry signals and GFP expression in different retinal layers, including photoreceptor (PR), outer nuclear layer (ONL), inner nuclear layer (INL), and retinal ganglion cell (RGC) layer (FIG. **4**B and FIG. **4**C). In addition, H&E staining of transverse retinal sections showed that cND-mC-C/C9 infusion did not affect retinal structure (FIG. **4**D). These findings suggest that cND-mC-C/C9 mixed with BSA represent a safe and effective retinal delivery system.

[0071] 2.4 Editing of Rs1 Gene by cND-mC-C/C9 in the Mouse Retina

[0072] We sought to investigate the efficiency and functional effects of genome editing by cND-mC-C/C9 nanoparticles in the mouse retina. Two linear DNA constructs, Rs1-sgRNA, encoding sgRNA and containing HDR template insert, as well as Cas9-GFP, encoding Cas9 endonuclease and GFP reporter, were designed to introduce c.625C>T mutation into the murine Rs1 gene (FIG. **5**A). These constructs were attached to cND-mC nanoparticles to produce cND-mC-C/C9, which in turn were injected into the mouse eyes. Two weeks after the injection, the percentage of edited alleles in retinal lysates was assessed by ddPCR, and was found to be about four times higher than the background signal detected in the retina of mice injected with cND-mC-C/C9 particles carrying Cas9-GFP construct only (FIG. **5**B). The fine anatomical structure of these retinas was observed by high-resolution OCT [36]. Whereas the retinas treated with cND-mC-C/C9 carrying Cas9-GFP construct only displayed the normally organized lamellar structure, the retinas treated with both constructs were characterized by highly undefined border between hyperreflective outer retinal bands 2 and 3, corresponding to ellipsoid region of photoreceptor inner segment (IS) and phagosome region of photoreceptor outer segment (OS), respectively (FIG. **5**C). The thickness of the combined hyperreflective outer retinal bands 2 and 3 was significantly reduced in Cas9+sgRNA treated retinas by approximately 30% (FIG. **5**D). Similarly, the H&E staining of the histology sections also revealed thickness reduction of IS/OS layer (FIG. **5**E and FIG. **5**F). In addition, the histology section showed loose outer nuclear layer (ONL) and inner nuclear layer (INL) structure, which was not evident from OCT images (FIG. **5**E). Taken together, our findings indicate that cND-mC-C/C9 treatment causes disruption in organization of photoreceptor layers (ONL, IS, and OS).

[0073] 2.5 Effect of cND-mC-C/C9-Mediated Rs1 Editing on Photoreceptor Cells in the Mouse Retina

[0074] To further study the effect of cND-mediated Rs1 gene editing on photoreceptors, we immunostained photoreceptor markers such as rhodopsin, cone cell-specific opsins, recoverin, and RS1 in the cross section of the mouse retinas. RS1 protein is normally expressed in photoreceptors and bipolar cells of the mouse retina [13]. Here, we observed that in the control retinas (treated with cND-mC-C/C9 carrying Cas9-GFP only), RS1 protein was enriched in the inner segment (IS) layer of the photoreceptors, but its localization was also extended to the outer nuclear layer (ONL), outer plexiform layer (OPL), and inner nuclear layer (INL) (FIG. **6**A, middle). On the other hand, the retinas treated with cND-mC-C/C9 particles carrying both CRISPR-Cas9 constructs were characterized by more concentrated localization in the IS layer and less spread to the other layers (FIG. **6**A, middle). Cone cell-specific opsins are normally localized in the outer segments of the cone cells and appear as linear and parallel signals in immunofluorescence staining imaging [37]. Indeed, such pattern of localization of cone cell-specific opsins was observed in the retinas treated with the control cND-mC-C/C9 (Cas9 only). On the contrary, retinas treated with Rs1-targeting cND-mC-C/C9 were characterized by significantly shorter and point-like appearance of opsin signal (FIG. **6**A and FIG. **6**C). Recoverin protein is known to be expressed in rod, cone, and bipolar cells, while rhodopsin is considered to be a marker

of rod cells [38-40]. The results of immunofluorescence staining showed that recoverin had significant immunoreactivity in the OPL, ONL, IS and OS of the control mouse retina (FIG. **6**B, left). In addition, rhodopsin had strong immunoreactivity in OS (FIG. **6**B, middle). The injection of Rs1-targeting cND-mC-C/C9 (Cas9+sgRNA) clearly caused more disordered localization of recoverin and rhodopsin in the IS/OS region, and in addition, the presence of the recoverin protein in the OPL was also irregular (FIG. **6**B, left).

[0075] In conclusion, the ND-based delivery system was designed to deliver the CRISPR-Cas9 components into human iPSCs and mouse retina. For this purpose, NDs were functionalized by adding carboxyl groups, which were used to attach mCherry protein and covalently link linear DNA encoding components of CRISPR-Cas9 system, including HDR template, sgRNA, Cas9 protein and GFP reporter. These NDs could be internalized by iPSCs and mouse retinas, and could introduce XLRS-specific mutation of RS1 gene. Mixing of NDs with BSA significantly increased the uptake by the cells. We demonstrated that the treatment of mouse retinas with CRISPR-Cas9-loaded NDs caused defects in organization of photoreceptor cells, which is a typical feature of XLRS. Therefore, we believe our ND-based strategy of genome editing has a great potential for establishing in vitro and in vivo disease models of XLRS (FIG. **7**).

[0076] While this specification contains many specifics, these should not be construed as limitations on the scope of the invention or of what may be claimed, but rather as descriptions of features specific to particular embodiments or examples of the invention. Certain features that are described in this specification in the context of separate embodiments or examples can also be implemented in combination in a single embodiment.

REFERENCES

[0077] [1] S. K. Sikkink, S. Biswas, N. R. Parry, P. E. Stanga, D. Trump, X-linked retinoschisis: an update, J Med Genet 44(4) (2007) 225-32.

[0078] [2] R. S. Molday, U. Kellner, B. H. Weber, X-linked juvenile retinoschisis: clinical diagnosis, genetic analysis, and molecular mechanisms, Prog Retin Eye Res 31(3) (2012) 195-212.

[0079] [3] A. Tantri, T. R. Vrabec, A. Cu-Unjieng, A. Frost, W. H. Annesley, Jr., L. A. Donoso, X-linked retinoschisis: a clinical and molecular genetic review, Sury Ophthalmol 49(2) (2004) 214-30.

[0080] [4] C. G. Sauer, A. Gehrig, R. Warneke-Wittstock, A. Marquardt, C. C. Ewing, A. Gibson, B. Lorenz, B. Jurklies, B. H. Weber, Positional cloning of the gene associated with X-linked juvenile retinoschisis, Nature genetics 17(2) (1997) 164-70.

[0081] [5] W. W. Wu, R. S. Molday, Defective discoidin domain structure, subunit assembly, and endoplasmic reticulum processing of retinoschisin are primary mechanisms responsible for X-linked retinoschisis, J Biol Chem 278(30) (2003) 28139-46.

[0082] [6] C. A. Curat, M. Eck, X. Dervillez, W. F. Vogel, Mapping of epitopes in discoidin domain receptor 1 critical for collagen binding, J Biol Chem 276(49) (2001) 45952-8.

[0083] [7] W. Vogel, Discoidin domain receptors: structural relations and functional implications, FASEB journal: official publication of the Federation of American Societies for Experimental Biology 13 Suppl (1999) S77-82.

[0084] [8] L. C. Eksandh, V. Ponjavic, R. Ayyagari, E. L. Bingham, K. T. Hiriyanna, S. Andreasson, B. Ehinger, P. A. Sieving, Phenotypic expression of juvenile X-linked retinoschisis in Swedish families with different mutations in the XLRS1 gene, Archives of ophthalmology (Chicago, Ill.: 1960) 118(8) (2000) 1098-104.

[0085] [9] Y. Inoue, S. Yamamoto, M. Okada, M. Tsujikawa, T. Inoue, A. A. Okada, S. Kusaka, Y. Saito, K. Wakabayashi, Y. Miyake, T. Fujikado, Y. Tano, X-linked retinoschisis with point mutations in the XLRS1 gene, Archives of ophthalmology (Chicago, Ill.: 1960) 118(1) (2000) 93-6.

[0086] [10] X. Li, X. Ma, Y. Tao, Clinical features of X linked juvenile retinoschisis in Chinese families associated with novel mutations in the RS1 gene, Molecular vision 13 (2007) 804-12.

[0087] [11] T. Wang, A. Zhou, C. T. Waters, E. O'Connor, R. J. Read, D. Trump, Molecular pathology of X linked retinoschisis: mutations interfere with retinoschisin secretion and oligomerisation, Br J Ophthalmol 90(1) (2006) 81-6.

[0088] [12] C. M. Mooy, L. I. Van Den Born, S. Baarsma, D. A. Paridaens, T. Kraaijenbrink, A. Bergen, B. H. Weber, Hereditary X-linked juvenile retinoschisis: a review of the role of Muller cells, Archives of ophthalmology (Chicago, Ill.: 1960) 120(7) (2002) 979-84.

[0089] [13] L. L. Molday, D. Hicks, C. G. Sauer, B. H. Weber, R. S. Molday, Expression of X-linked retinoschisis protein RS1 in photoreceptor and bipolar cells, Investigative ophthalmology & visual science 42(3) (2001) 816-25.

[0090] [14] S. N. Reid, C. Yamashita, D. B. Farber, Retinoschisin, a photoreceptor-secreted protein, and its interaction with bipolar and muller cells, The Journal of neuroscience: the official journal of the Society for Neuroscience 23(14) (2003) 6030-40.

[0091] [15] Z. Y. Lien, T. C. Hsu, K. K. Liu, W. S. Liao, K. C. Hwang, J. I. Chao, Cancer cell labeling and tracking using fluorescent and magnetic nanodiamond, Biomaterials 33(26) (2012) 6172-85.

[0092] [16] K. K. Liu, C. C. Wang, C. L. Cheng, J. I. Chao, Endocytic carboxylated nanodiamond for the labeling and tracking of cell division and differentiation in cancer and stem cells, Biomaterials 30(26) (2009) 4249-59.

[0093] [17] L. Moore, J. Yang, T. T. Lan, E. Osawa, D. K. Lee, W. D. Johnson, J. Xi, E. K. Chow, D. Ho, Biocompatibility Assessment of Detonation Nanodiamond in Non-Human Primates and Rats Using Histological, Hematologic, and Urine Analysis, ACS Nano 10(8) (2016) 7385-400.

[0094] [18] C. C. Fu, H. Y. Lee, K. Chen, T. S. Lim, H. Y. Wu, P. K. Lin, P. K. Wei, P. H. Tsao, H. C. Chang, W. Fann, Characterization and application of single fluorescent nanodiamonds as cellular biomarkers, Proceedings of the National Academy of Sciences of the United States of America 104(3) (2007) 727-32.

[0095] [19] X. Q. Zhang, M. Chen, R. Lam, X. Xu, E. Osawa, D. Ho, Polymer-functionalized nanodiamond platforms as vehicles for gene delivery, ACS Nano 3(9) (2009) 2609-16.

[0096] [20] H. L. Chu, H. W. Chen, S. H. Tseng, M. H. Hsu, L. P. Ho, F. H. Chou, M. P. Li, Y. C. Chang, P. H. Chen, L. Y. Tsai, C. C. Chou, J. S. Chen, T. M. Cheng, C. C. Chang, Development of a growth-hormone-conjugated nanodiamond complex for cancer therapy, ChemMedChem 9(5) (2014) 1023-9.

[0097] [21] C. Y. Cheng, E. Perevedentseva, J. S. Tu, P. H. Chung, C. L. Cheng, K. K. Liu, J. I. Chao, P. H. Chen, C. C. Chang, Direct and in vitro observation of growth hormone receptor molecules in A549 human lung epithelial cells by nanodiamond labeling, Applied Physics Letters 90(16) (2007).

[0098] [22] M. G. Chernysheva, I. Y. Myasnikov, G. A. Badun, Myramistin adsorption on detonation nanodiamonds in the development of drug delivery platforms, Diamond and Related Materials 55 (2015) 45-51.

[0099] [23] V. N. Mochalin, A. Pentecost, X. M. Li, I. Neitzel, M. Nelson, C. Wei, T. He, F. Guo, Y. Gogotsi, Adsorption of drugs on nanodiamond: toward development of a drug delivery platform, Mol Pharm 10(10) (2013) 3728-35.

[0100] [24] K. Turcheniuk, V. N. Mochalin, Biomedical applications of nanodiamond (Review), Nanotechnology 28(25) (2017) 252001.

[0101] [25] H. S. Choi, W. Liu, P. Misra, E. Tanaka, J. P. Zimmer, B. Itty Ipe, M. G. Bawendi, J. V. Frangioni, Renal clearance of quantum dots, Nat Biotechnol 25(10) (2007) 1165-70.

[0102] [26] Z. U. Hasan, P. R. Hemmer, H. Lee, A. L. Migdall, O. Shenderova, N. Nunn, T. Oeckinghaus, M. Torelli, G. McGuire, K. Smith, E. Danilov, R. Reuter, J. Wrachtrup, A. Shames, D. Filonova, A. Kinev, Commercial quantities of ultrasmall fluorescent nanodiamonds containing color centers, Advances in Photonics of Quantum Computing, Memory, and Communication X, 2017.

[0103] [27] F. C. Barone, C. Marcinkiewicz, J. Li, M. Sternberg, P. I. Lelkes, D. A. Dikin, P. J. Bergold, J. A. Gerstenhaber, G. Feuerstein, Pilot study on biocompatibility of fluorescent nanodiamond-(NV)-Z-800 particles in rats: safety, pharmacokinetics, and bio-distribution (part III), Int J Nanomedicine 13 (2018) 5449-5468.

[0104] [28] K. Purtov, A. Petunin, E. Inzhevatkin, A. Burov, N. Ronzhin, A. Puzyr, V. Bondar, Biodistribution of Different Sized Nanodiamonds in Mice, Journal of Nanoscience and Nanotechnology 15(2) (2015) 1070-1075.

[0105] [29] E. Perevedentseva, Y. C. Lin, M. Jani, C. L. Cheng, Biomedical applications of nanodiamonds in imaging and therapy, Nanomedicine (Lond) 8(12) (2013) 2041-60.

[0106] [30] M. Yu, J. Zheng, Clearance Pathways and Tumor Targeting of Imaging Nanoparticles, ACS Nano 9(7) (2015) 6655-74.

[0107] [31] E. R. Burnight, M. Gupta, L. A. Wiley, K. R. Anfinson, A. Tran, R. Triboulet, J. M. Hoffmann, D. L. Klaahsen, J. L. Andorf, C. Jiao, E. H. Sohn, M. K. Adur, J. W. Ross, R. F. Mullins, G. Q. Daley, T. M. Schlaeger, E. M. Stone, B. A. Tucker, Using CRISPR-Cas9 to Generate Gene-Corrected Autologous iPSCs for the Treatment of Inherited Retinal Degeneration, Mol Ther 25(9) (2017) 1999-2013.

[0108] [32] J. H. Chuang, A. A. Yarmishyn, D. K. Hwang, C. C. Hsu, M. L. Wang, Y. P. Yang, K. H. Chien, S. H. Chiou, C. H. Peng, S. J. Chen, Expression profiling of cell-intrinsic regulators in the process of differentiation of human iPSCs into retinal lineages, Stem Cell Res Ther 9(1) (2018) 140.

[0109] [33] P. H. Chen, C. H. Wu, Y. F. Chen, Y. C. Yeh, B. H. Lin, K. W. Chang, P. Y. Lai, M. C. Hou, C. L. Lu, W. C. Kuo, Combination of structural and vascular optical coherence tomography for differentiating oral lesions of mice in different carcinogenesis stages, Biomed Opt Express 9(4) (2018) 1461-1476.

[0110] [34] Y. K. Tzeng, O. Faklaris, B. M. Chang, Y. Kuo, J. H. Hsu, H. C. Chang, Superresolution imaging of albumin-conjugated fluorescent nanodiamonds in cells by stimulated emission depletion, Angew Chem Int Ed Engl 50(10) (2011) 2262-5.

[0111] [35] K.-i. Hanaki, A. Momo, T. Oku, A. Komoto, S. Maenosono, Y. Yamaguchi, K. Yamamoto, Semiconductor quantum dot/albumin complex is a long-life and highly photostable endosome marker, Biochemical and Biophysical Research Communications 302(3) (2003) 496-501.

[0112] [36] J. P. Syu, W. Buddhakosai, S. J. Chen, C. C. Ke, S. H. Chiou, W. C. Kuo, Supercontinuum source-based multi-contrast optical coherence tomography for rat retina imaging, Biomed Opt Express 9(12) (2018) 6132-6144.

[0113] [37] Y. Liang, D. Fotiadis, T. Maeda, A. Maeda, A. Modzelewska, S. Filipek, D. A. Saperstein, A. Engel, K. Palczewski, Rhodopsin signaling and organization in heterozygote rhodopsin knockout mice, J Biol Chem 279(46) (2004) 48189-96.

[0114] [38] A. H. Milam, D. M. Dacey, A. M. Dizhoor, Recoverin immunoreactivity in mammalian cone bipolar cells, Visual neuroscience 10(1) (1993) 1-12.

[0115] [39] K. Sakurai, J. Chen, S. C. Khani, V. J. Kefalov, Regulation of mammalian cone phototransduction by recoverin and rhodopsin kinase, J Biol Chem 290(14) (2015) 9239-50.

[0116] [40] K. Szabo, A. Szabo, A. Enzsoly, A. Szel, A. Lukats, Immunocytochemical analysis of misplaced rhodopsin-positive cells in the developing rodent retina, Cell and tissue research 356(1) (2014) 49-63.

SEQUENCE LISTING

<160> NUMBER OF SEQ ID NOS: 13

<210> SEQ ID NO 1
<211> LENGTH: 96
<212> TYPE: DNA
<213> ORGANISM: Artificial Sequence
<220> FEATURE:
<223> OTHER INFORMATION: Synthetic

-continued

<400> SEQUENCE: 1

ggcacgtctg cattgccatc gttttagagc tagaaatagc aagttaaaat aaggctagtc 60

cgttatcaac ttgaaaaagt ggcaccgagt cggtgc 96

<210> SEQ ID NO 2
<211> LENGTH: 190
<212> TYPE: DNA
<213> ORGANISM: Artificial Sequence
<220> FEATURE:
<223> OTHER INFORMATION: Synthetic

<400> SEQUENCE: 2

gtcttctatg gcaactcgga ccgcacctcc acggttcaga acctgctgcg gccccccatc 60

atctcccgct tcatccgcct catcccgctg ggctggcatg tccggattgc catccggatg 120

gagctgctgg agtgcgtcag caagtgtgcc tgatgcctgc ctcagctcgg cgcctgccag 180

ggggtgactg 190

<210> SEQ ID NO 3
<211> LENGTH: 96
<212> TYPE: DNA
<213> ORGANISM: Artificial Sequence
<220> FEATURE:
<223> OTHER INFORMATION: Synthetic

<400> SEQUENCE: 3

ggcatgtccg aattgccatc gttttagagc tagaaatagc aagttaaaat aaggctagtc 60

cgttatcaac ttgaaaaagt ggcaccgagt cggtgc 96

<210> SEQ ID NO 4
<211> LENGTH: 190
<212> TYPE: DNA
<213> ORGANISM: Artificial Sequence
<220> FEATURE:
<223> OTHER INFORMATION: Synthetic

<400> SEQUENCE: 4

gtcttctatg gaaactcaga ccggagttct acagttcaga acttactcag gccccccatc 60

atttcccgct tcatccgact gatccctcta ggctggcacg tctgtattgc catccggatg 120

gagctgcttg agtgtgccag caagtgtgcc tgatgtctat ttcagctcag ttctgtcact 180

tgcagggaga 190

<210> SEQ ID NO 5
<211> LENGTH: 12
<212> TYPE: DNA
<213> ORGANISM: Artificial Sequence
<220> FEATURE:
<223> OTHER INFORMATION: Synthetic

<400> SEQUENCE: 5

cgtccgcatt gc 12

<210> SEQ ID NO 6
<211> LENGTH: 12
<212> TYPE: DNA
<213> ORGANISM: Artificial Sequence
<220> FEATURE:
<223> OTHER INFORMATION: Synthetic

-continued

<400> SEQUENCE: 6

cgtctgcatt gc 12

<210> SEQ ID NO 7
<211> LENGTH: 32
<212> TYPE: DNA
<213> ORGANISM: Artificial Sequence
<220> FEATURE:
<223> OTHER INFORMATION: Synthetic

<400> SEQUENCE: 7

cgctgggctg gcacgtccgc attgccatcc gg 32

<210> SEQ ID NO 8
<211> LENGTH: 32
<212> TYPE: DNA
<213> ORGANISM: Artificial Sequence
<220> FEATURE:
<223> OTHER INFORMATION: Synthetic

<400> SEQUENCE: 8

ccggatggca atacggacat gccagcccag cg 32

<210> SEQ ID NO 9
<211> LENGTH: 20
<212> TYPE: DNA
<213> ORGANISM: Artificial Sequence
<220> FEATURE:
<223> OTHER INFORMATION: Synthetic

<400> SEQUENCE: 9

ggcacgtctg cattgccatc 20

<210> SEQ ID NO 10
<211> LENGTH: 32
<212> TYPE: DNA
<213> ORGANISM: Artificial Sequence
<220> FEATURE:
<223> OTHER INFORMATION: Synthetic

<400> SEQUENCE: 10

ctctaggctg gcatgtccga attgccatcc gg 32

<210> SEQ ID NO 11
<211> LENGTH: 32
<212> TYPE: DNA
<213> ORGANISM: Artificial Sequence
<220> FEATURE:
<223> OTHER INFORMATION: Synthetic

<400> SEQUENCE: 11

ccggatggca attcggacat gccagcctag ag 32

<210> SEQ ID NO 12
<211> LENGTH: 20
<212> TYPE: DNA
<213> ORGANISM: Artificial Sequence
<220> FEATURE:
<223> OTHER INFORMATION: Synthetic

<400> SEQUENCE: 12

ggcatgtccg aattgccatc 20

-continued

<210> SEQ ID NO 13
<211> LENGTH: 20
<212> TYPE: DNA
<213> ORGANISM: Artificial Sequence
<220> FEATURE:
<223> OTHER INFORMATION: Synthetic

<400> SEQUENCE: 13

ccgtacaggc ttaacggtag 20

What is claimed is:

1. A delivery system for gene editing comprising nanodiamond (ND) particles as the carriers of CRISPR-Cas9 components including a Cas9 protein, a guide protein (gRNA), a template DNA designed to introduce the mutation in a given gene for repairing a tissue damage, wherein the ND particles have a diameter less than 5 nm, and functionalized by carboxylation of the surface and covalently conjugated with a fluorescent protein: and a first linear DNA construct for expression of the Case 9 protein, and a second, linear DNA construct for expression of the gRNA/template DNA were linked with the ND particles covalently conjugated with the fluorescent protein by phosphoryl imidazole to obtain carboxylated nanodiamond-mediated CRISPR-Cas9 particles.

2. The system of claim **1**, wherein the ND particles have a diameter in a range of 3 nm-5 nm.

3. The system of claim **1**, wherein the ND particles have a diameter of about 3 nm.

4. The system of claim **1**, wherein the fluorescent protein is a mCherry protein.

5. The system of claim **1**, which the particles are coated by bovine serum albumin (BSA) before using.

6. The system of claim **1**, wherein the given gene is RS1 gene associated with X-linked retinoschisis (XLRS).

7. The system of claim **6**, which is used as a tool for creating an in vitro and in vivo disease model of XLRS.

8. The system of claim **6**, wherein the mutation in the given gene is introduced via two linear DNA constructs, which are attached to the conjugated mCherry, and the first linear DNA construct encodes for Cas9 endonuclease and a green fluorescent protein (GFP) reporter, and the second linear DNA construct encodes for a sgRNA and contains an insert of HDR template designed to introduce RS1 c.625C>T mutation.

9. The system of claim **7**, wherein the delivery leads to introduction of RS1 c.625C>T mutation in human iPSCs or mouse retinas.

10, A method for treating a disease or repairing a tissue damage in a subject, comprising delivering and internalizing the mutation in a given gene into said subject through the system of claim **1**.

11. The use of claim **10**, wherein the disease is X-linked retinoschisis (XLRS).

12. The use of claim **11**, wherein the given gene is RS1 gene associated with X-linked retinoschisis (XLRS).

13. A method for creating an in vitro or in vivo disease model, comprising delivering and internalizing the mutation in a given gene into induced pluripotent stem cells (iPSCs) or an animal organ through the system of claim **1**,

14. The method of claim **13**, wherein the disease is X-linked retinosehisis (XLRS).

15. The method of claim **14**, wherein the given gene is RS1 gene associated with X-linked retinoschisis (XLRS).

16. The method of claim **14**, wherein the animal organ is mouse retinas.

17. The method of claim **15**, wherein the delivery leads to an introduction of RS1 c.625C>T mutation into human iPSCs or mouse retinas.

18. The method of claim **16**, wherein the Rs1 gene editing in the mouse retinas results in several pathological features typical for XLRS.

19. The method of claim **18**, wherein the pathological feature typical for XLRS is aberrant photoreceptor structure.

* * * * *